THE ROLE OF CALCIUM IN THE MALPIGHIAN TUBULES OF THE KISSING BUG *Rhodnius prolixus*

A Thesis Submitted to the College of

Graduate Studies and Research

In Partial Fulfillment of the Requirements

For the Degree of Master of Science

In the Department Physiology

University of Saskatchewan

Saskatoon

by

PAULA GIOINO

PERMISSION TO USE:

In presenting this thesis in partial fulfillment of the requirements for a of Master of Science degree from the University of Saskatchewan, I agree that the Libraries of this University may make it freely available for inspection. I further agree that permission for copying of this thesis/dissertation in any manner, in whole or in part, for scholarly purposes may be granted by the professor or professors who supervised my thesis/dissertation work or, in their absence, by the Head of the Department or the Dean of the College in which my thesis work was done. It is understood that any copying or publication or use of this thesis/dissertation or parts thereof for financial gain shall not be allowed without my written permission. It is also understood that due recognition shall be given to me and to the University of Saskatchewan in any scholarly use which may be made of any material in my thesis.

Requests for permission to copy or to make other uses of materials in this thesis/dissertation in whole or part should be addressed to one of the following:

Head of the Department of Physiology
University of Saskatchewan,
107 Wiggins Road, Saskatoon, Saskatchewan,
S7N 5E5
Canada

OR

Dean of the College of Graduate Studies and Research
University of Saskatchewan
107 Administration Place, Saskatoon,
Saskatchewan, S7N 5A2, Canada

ABSTRACT:

Stimulation of urine production by the Malpighian (renal) tubules in *Rhodnius prolixus* is regulated by at least two diuretic hormones, CRF-related peptide and serotonin, that have traditionally been believed to function through the activation of cAMP-mediated intracellular second messenger pathways. In this study I demonstrate that serotonin stimulation triggered, in addition to cAMP, intracellular Ca^{2+} waves in the Malpighian tubule cells of *R. prolixus*. Treatment with the intracellular Ca^{2+} chelator BAPTA-AM blocked the intracellular Ca^{2+} waves and reduced serotonin-stimulated fluid secretion by 75%. This suggests a role for intracellular Ca^{2+} signaling in the excretory system of *R. prolixus*. Serotonin stimulated Malpighian tubules (MTs) exposed to Ca^{2+}-free saline plus BAPTA-AM secreted an abnormal fluid, showing: increased K^+ concentration, reduced Na^+ concentration and lower pH. These results along with measurement of transepithelial potential (TEP) suggest that the basolateral Na^+:K^+:2Cl^- cotransporter (NKCC) activity is reduced in tubule cells treated with BAPTA-AM, suggesting that Ca^{2+} is required to modulate the activity of the basolateral NKCC.

Treatment with the non-hydrolysable cell-permeable cAMP analog, 8Br-cAMP, produced fluid with the same K^+ and Na^+ concentration and at the same secretion rate as serotonin-stimulated tubules. In addition, 8Br-cAMP triggered intracellular Ca^{2+} oscillations similar to those obtained with serotonin. 8Br-cAMP-stimulated tubules treated with BAPTA-AM decreased their fluid secretion by about 40% and increased Na^+ concentration, similar to the effect observed on serotonin-stimulated tubules. Therefore, I conclude that the intracellular Ca^{2+} waves triggered by serotonin are mediated by cAMP.

The role of inositol-3-phospate (InsP3) in Ca^{2+} release was tested by treating the tubules with the InsP3 receptor blocker xestospongin. The treatment decreased fluid secretion rate as

well as the amplitude of Ca^{2+} waves in serotonin-stimulated tubules. These results suggest that serotonin activates the production of InsP3 and, most likely, diacylglycerol (DAG). Thus, I decided to test whether the protein kinase C (PKC) may be involved in serotonin-stimulated secretion.

The PKC inhibitors chelerythrine and bisindolylmaleimide (BIM) decreased secretion fluid rate in serotonin-stimulated tubules by 50% and 70%, respectively. Fluid secreted by tubules treated with BIM showed no differences in K^+ and Na^+ concentrations compared to controls, however both ion fluxes decreased. The evidence suggests that PKC is involved in serotonin stimulated secretion; the mechanism is still not understood.

Taken together, the results suggest that cAMP, Ca^{2+} and PLC-PKC pathway are involved in serotonin stimulated secretion. However cAMP stimulation is enough for maximal secretion rate. Therefore PLC-PKC must act downstream of cAMP. Based on those results we hypothesize that serotonin binds a GPCR, increasing cAMP by activation of an adenylate cyclase (AC). Subsequently, cAMP is somehow able to activate PLC, which finally produces Ca^{2+} release, PKC activation and NKCC upregulation.

ACKNOWLEGMENTS:

I would like to say ‘muchas gracias’ my supervisor Dr. Juan Ianowski for giving me the opportunity to come to this University and work under his supervision. It has been a pleasure to work with him.

Thanks to my advisory committee members Nigel West and Michel Desautels for their contributions, suggestions and, specially, for making me feel so comfortable during our meetings.

Enormous thanks to my husband Bernardo, who came all the way from Argentina just for me to do this Master and gave me his support during all this time.

To my family, who supported me in every decision I’ve taken in my life; mom for listening to me during my crisis periods, Seba for solving so many issues I had back there in Argentina and Silvia, my mother in law, for being so positive and considerate.

One “muchas gracias chichis” to my best friends Vale, Male, Geo and Maria, whom I miss and love, for their multiple suggestions and advice. A huge thanks to Jay and Emma, for the company and laboratory laughs.

Finally, to the University of Saskatchewan for accepting me and to all the animals I used during my experiments, which contributed with their life to this study.

LIST OF CONTENTS:

LIST OF FIGURES

LIST OF ABBREVIATIONS:

AC: Adenylate cyclase

BIM: bisindolylmaleimide-I

CRF: corticotrophin-releasing factor

DAG: diacylglycerol

DMSO: Dimethyl sulfoxide

Epac: exchange protein activated by cAMP

InsP3: Inositol trisphosphate

InsP3R: Inositol trisphosphate receptor

JUNK: c-Jun N-terminal kinase

MTs: Malpighian tubules

NKCC: Na^+:K^+:2Cl^- cotransporter

OSR1: Oxidative stress response 1

p38: P38 mitogen-activated protein kinase

PKA: protein kinase A

PKC: protein kinase C

RyR: Ryanodine receptor

SPAK: Ste20-related proline alanine-rich kinase

TEP: transepithelial potential

V-ATPase: V-type H^+-ATPase

WNK: with no lysine kinase

1. INTRODUCTION:

1.1. General introduction to insects

1.1.1 Insect anatomy

"Insect," from Latin insectum, means "cut into sections". This is the most diverse and large group of animals and is contained within the phylum arthropoda. The body of insects is divided into head, thorax and abdomen. The head is an unsegmented unit which contains the sensory organs like antennae, eyes and mouthparts. The thorax is divided into three sections that run from head to abdomen: prothorax, mesothorax and metathorax. There are three pairs of legs in the thorax; one pair per segment. The legs may be specialized for different tasks. In mantises, for example, the two prothoracic legs are spiked in order to catch and hold prey. From the meso and metathorax segments of most insects two pairs of wings emerge. The abdomen unit consists of 11-12 segments that can be fused together. The abdomen contains the heart, the reproductive, digestive and excretory organs [1,2].

1.1.2. Development

Insects present a rigid exoskeleton or cuticle, mainly made of chitin, that limits growth. Therefore, development involves different discrete stages and, transition from one stage to the other requires the complete renewal of the cuticle and cuticular lining [3].

Immature stages in insects differ from adults, and there are two groups of insects based on the metamorphosis process: (I) Holometabolous insects; which undergo complete metamorphosis and, (II) hemimetabolous insects; which, on the other hand, undergo an

incomplete metamorphosis. The typical example of a holometabolous insect is the butterfly. The worm-like larvae hatch from the eggs and feed on plants. The larvae develop into a pupa stage, sealed within the cocoon, until the imago or adult butterfly ecloses from the pupa and feeds on nectar. In contrast, hemimetabolous insects do not have a pupal stage and the nymphs (i.e. juveniles) stages are anatomically, physiologically and ecologically similar to adults stages except that they lack wings and a developed reproductive system [2,4,5].

R. prolixus is a blood sucking insect, vector of Chagas' disease; a condition that causes 45,000-50,000 deaths/year. *R. prolixus* are hemimetabolous insects with 5 nymphal stages (instars) before reaching adulthood. The complete life cycle requires from 3 months up to 2 years depending on the environmental conditions; where access to hosts, ambient temperature, humidity and light cycle are key factors in hatching from the egg and molting from one nymph stage to the other [6]. Initiation of molting and reproduction are processes hormonally regulated and in this subfamily the blood meal triggers both events [2,7].

1.1.3. Physiology

1.1.3.1. Circulatory and respiratory system

The insect's respiratory system consists of a network of internal air tubes, called tracheae, that deliver O_2 to the tissues and retrieves CO_2. Trachea branch into smaller tubes called tracheoles where O_2 and CO_2 diffuse to and from the tissues [4] At the end of the tracheoles there are flexible blind-ended structures called air sacs. These air sacs can expand or collapse due to the abdominal muscle movements that exert negative or positive pressure on the hemolymph and subsequently on the air sacs. This creates a convective movement of gases. The respiratory system in insects allows some species (i.e flying insects) to reach very high metabolic rates,

higher than in mammals [8–10]. However, the tracheal system limits the size of the animals since the larger the insect, the more volume is occupied by the tracheal system. Thus, beyond a certain size, the tracheal system starts to interfere with other body functions [1].

Insects have an open circulatory system where the organs are bathed with the insect's blood, the hemolymph, within the body cavity, i.e. the hemocoel. A single dorsal blood vessel runs from the anterior to the posterior end of the hemocoel. The anterior segment of the dorsal vessel, called the aorta, lacks valves or musculature. The posterior segment, called the heart, is contractile pump that drives hemolymph flow towards the anterior segments of the animal. Subsequently the hemolymph flows back to the posterior part of the body where the cycle repeats. The main function of this system is to transport nutrients, waste products, hormones and components of the immune system. Is important to point out that this system is not involved in oxygen distribution since usually there is no oxygen transport protein in it. However, a few insects contain the oxygen transport protein hemocyanin [11].

1.1.3.2. The excretory system

In insects, the excretory function is carried out by two organs, the alimentary canal and the Malpighian (renal) tubules.

The alimentary canal is divided in three regions, the foregut, midgut and hindgut. The foregut and the midgut in the alimentary canal are separated by the stomodeal or cardiac valve that prevents the back flow of material. In *R. prolixus* the midgut has an enlarged region, the crop, that stores the ingested blood meal and occupies a large space in the hemocoel. From the crop the plasma fraction of the blood meal is transported into the hemolymph (see Fig. 1). This extra volume that is then excreted by the Malpighian (renal) tubules as urine. Malpighian

tubules are long blind-ended tubular structures that emerge from the midgut at the junction with the hindgut. The number and length of the Malpighian tubules varies among insect groups. In *R. prolixus*, there are 4 Malpighian tubules, each about 100 µm in diameter and 45mm in length [12,13]. Malpighian tubules are divided into two segments; the proximal segment that is directly attached to the alimentary canal and the distal segment that is about two thirds of the entire tubule.

The lack of a closed circulatory system makes it impossible to create primary urine by ultrafiltration due to the lack of blood pressure to drive this process. Thus, insects create urine by active ion transport and water flow by osmosis across the Malpighian tubules. The distal segment of Malpighian tubules actively transport fluid into the lumen of the tubule producing a primary urine. The primary urine flows into the proximal segment where K^+ and Cl^- are reabsorved forming the final urine. The final urine, along with feces, is finally excreted from the hingut (Fig. 1).

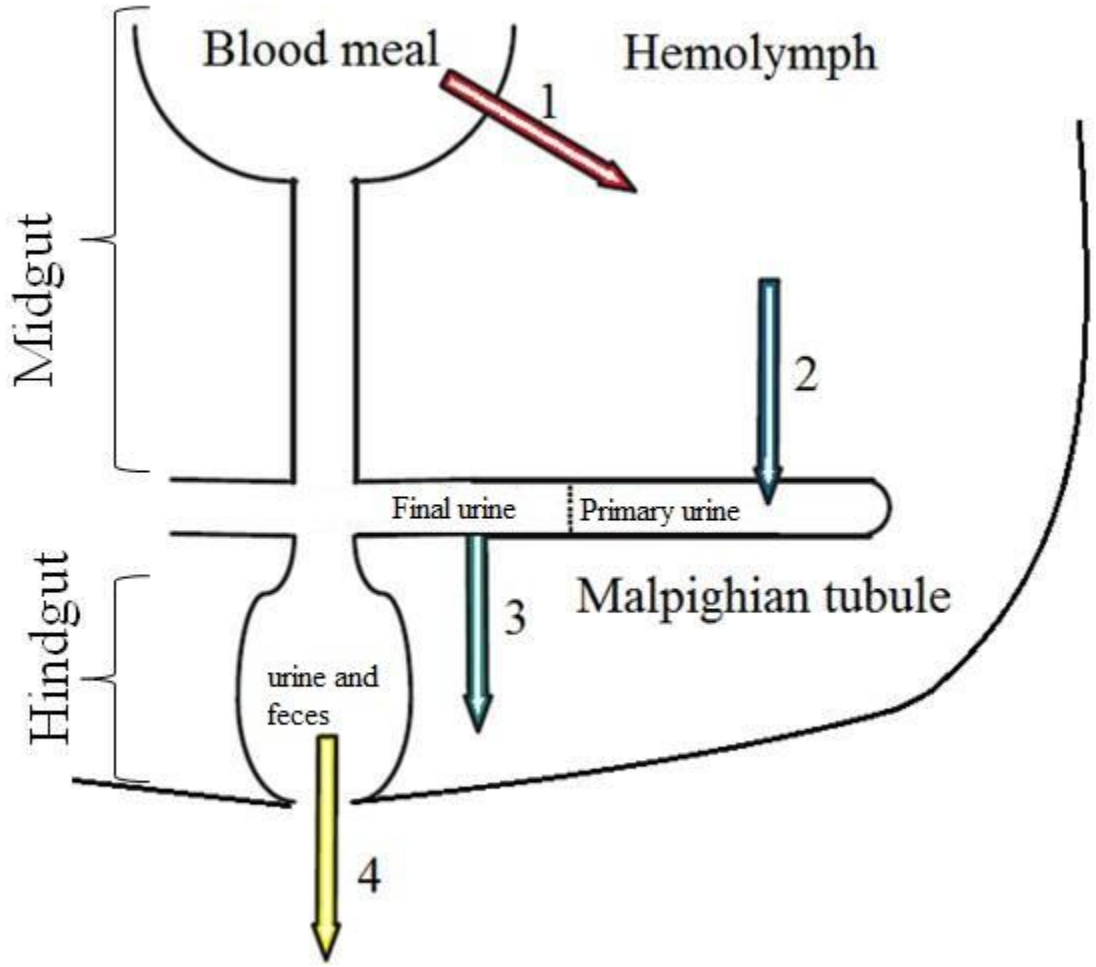

Figure 1: Cartoon representing the excretory system. The blood meal is stored in the crop where it is concentrated. For that, the plasma fraction of the blood meal is transported into the hemolymph (1) and later into the lumen of the distal segment of the Malpighian tubules as primary urine (2). Urine is then modified in the proximal segment by reabsortion of K^+ an Cl^- into the hemolymph, forming the final urine (3). Final urine flows to the hindgut where it is excreted, along with feces, out of the system (4).

1.1.3.3. The stress of a meal

Blood meals in *R. prolixus* are infrequent but abundant. In approximately 15 minutes nymphs can ingest the equivalent to 10 times their own unfed body weight in blood [14]. The blood meal is so large that it requires the animal to modify the properties of the exoskeleton. Therefore, to accommodate the ingested volume, the insect cuticle becomes more extensible [15].

The increase in body weight and size after the blood meal restricts the insect's maneuverability, increasing the risk of predation. Furthermore, *R. prolixus* feeds on blood that is hypo-osmotic to its own hemolymph. Therefore, the meal poses a considerable threat to homeostasis. Thus, these insects undergo a rapid postprandial diuresis that allows the excretion of 50% of the volume ingested in 2hrs [16].

The rapid diuresis is initiated by stretch receptors in the cuticle that trigger the release of diuretic hormones [15]. Two diuretic hormones, corticotropin-releasing factor (CRF)-related peptide and serotonin, are released into the hemolymph and stimulate the crop and Malpighian tubules to produce urine. Both hormones stimulate the formation of primary urine by the distal segment via transpithelial active transport of K^+, Cl^- and Na^+ ions [17,18]. Ion transport by the the Malpighian tubules of *R. prolixus* is thought the cell (transcellular transport), while movement of solutes and water between cells (paracellular transport) is minimal [19].

The current model for ion transport in distal Malpighian tubule cells of *R. prolixus* proposes that an apical vacuolar-type H^+-ATPase energizes transport by generating a H^+ gradient across the apical membrane. This H^+ gradient is dissipated by Na^+/H^+ and/or K^+/H^+ exchangers that mediate the movement of Na^+ and K^+ into the lumen while Cl^- crosses the apical membrane through channels. The entry across the basolateral membrane of K^+, Cl^- and Na^+ ions is mediated by a bumetanide-sensitive NKCC (Fig. 2) [20–22]. The cell membranes of the Malpighian tubule

cells are highly permeable to water, most likely due to the expression of aquaporins [19,23]. This allows water to follow a small osmotic gradient generated by the active transport of ions from the hemolymph into the lumen of the tubule, thus forming primary urine [19]. Fully stimulated Malpighian tubule cells transport ions at massive rates equivalent to each cell exchanging their intracellular Na^+ and Cl^- content in 3-5 sec and whole cell volume every 10-15 sec [24,25]. In the absence of regulatory mechanisms the Malpighian tubules would deplete the entire hemolymph K^+ content in just 1 min [26,27]. Thus, ion transport by the Malpighian tubules is precisely regulated by the diuretic hormones, CRF-related peptide and serotonin, and the antidiuretic hormone, RoprCAPA2, that have been shown to modulate ion transport though cAMP intracellular second messenger pathways. Calcium is believed to play no significant role as a second messenger in Malpighian tubules of *R. prolixus* during diuresis [28]. However, Ca^{2+} plays a major role in regulating the Malpighian tubules in many other insect species. Thus, I tested the role of Ca^{2+} in serotonin-stimulated Malpighian tubules from *R. prolixus*.

1.2. *Rhodnius prolixus* and Chagas' disease

Chagas' disease was first described by Carlos Chagas in 1909 and currently affects 11 million people in the Americas [6,29]. Chagas' disease is caused by the parasite *Trypanosome cruzi* affecting various internal organs; however most of the mortality is caused by heart failure. There are different modes of Chagas' transmission, but most commonly infection occurs through the feces of blood sucking insects from the subfamily Triatominae. The most important vector species of Chagas' disease are *R. prolixus* and *Triatoma infestans*, commonly known as kissing bugs. These insects deposit infected feces on the skin of the human host during a blood meal, allowing the parasite to enter the blood stream through the skin or bite wound [30]. Currently there

is no treatment or vaccine for the disease. Thus, the prevention strategy is to control the vector population with insecticides. However, the use of such pesticides has created resistant vector populations, leading to re-infestations of large areas. In order to completely eliminate the vector from populated regions, researchers have been studying the physiology and biology of *R. prolixus* and *T. infestans* for the last seven decades [6].

1.2.1. *R. prolixus* is a vector of Chagas' disease

All vector species of Chagas' disease are within the insect group Heteroptera. The Heteroptera, or "true bugs", are comprised by about 50,000 diverse species of insects. A main characteristic of Heteroptera is a piercing-sucking mouthpart that is used to extract the fluid from plants or animals, but only a small number of species within this group feed on vertebrate blood. The only Heteroptera species of public health concern are kissing bugs and bed bugs [6]. Most Canadians have at least heard of the existence of bed bugs, and probably understand the reason for the popular name. Kissing bugs, however, are not so abundant in North America (Mexico and southern United States) and the origin of the name is not that evident. Most domiciliary kissing bugs don't live in mattresses as bed bugs do, but in cracks on the walls and straw ceiling of human dwellings, where they take refuge during the day. At night, when their hosts are inactive, kissing bugs detect diverse signals such as, temperature and CO_2 exhaled from the host, that attract the insects to the face and mouth area where most bites occur, thus the name "kissing bug" [31].

1.3 Objectives

Based that in many epithelial tissues Ca^{2+} is involved in ion transporters regulation [32–35] and that in insects Ca^{2+} is known to play a role in the secretory process of Malpighian tubules [36–42]; I propose the hypothesis that Ca^{2+} plays a key role in the modulation of transporters during diuresis in the Malpighian tubules of R. prolixus

Therefore, the main goal of this thesis is to re-assess the role of intracellular Ca^{2+} signaling in *R. prolixus* Malpighian tubules during diuresis [28].

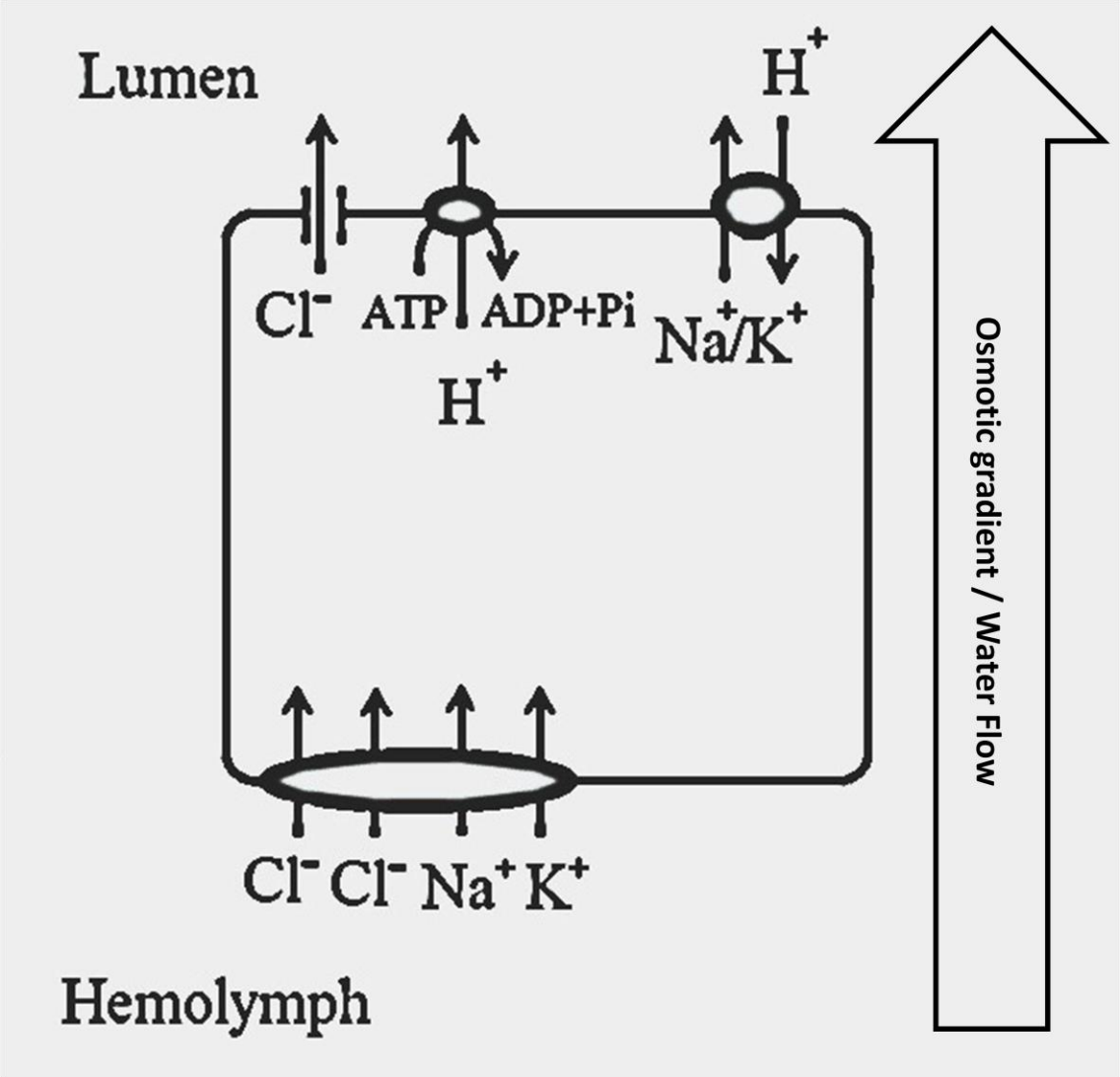

Figure 2: Proposed model for Malpighian tubule cell secretion in *R. prolixus*. The apical V-ATPase creates a H^+ gradient across the apical membrane that is dissipated by Na^+/H^+ and/or K^+/H^+ exchangers. Following the generated driving force, Na^+, K^+ and Cl^- enter across the basolateral bumetanide-sensitive NKCC. Cl^- exits the cell via an apical channel. Water follows a small osmotic gradient; the lumen is slightly hypertonic to the cell, and the cell is slightly hypertonic to the hemolymph.

1.3.1. Calcium signaling

The intracellular mechanisms that regulate secretion in Malpighian tubules of insects are still uncertain. However, in many species diuretic hormones seem to trigger intracellular Ca^{2+} signaling. In the house cricket *Acheta domesticus*, serotonin is a diuretic stimulus that promotes Ca^{2+} release from intracellular stores[40]. In other insects, including *Aedes aegypti* [41], *Anopheles stephensi* and *Anopheles gambiae* [42], the hormone leucokinin induces Malpighian tubule secretion via Ca^{2+} signaling. In *Drosophila melanogaster* Malpighian tubules, leucokinin and CAP2b [43] increase cytosolic Ca^{2+} via InsP3Rs [36]. In contrast, a role for Ca^{2+} in the Malpighian tubules of *R. prolixus* has been rejected on the basis that chelating extracellular Ca^{2+} with EGTA and treatment with the intracellular Ca^{2+} antagonist TMB-8 does not block serotonin-stimulated secretion[44,45]. Given that Ca^{2+} seems to be a conserved mechanism for regulation Malpighian tubule function we tested the role of Ca^{2+} in *R. prolixus* tubules.

2. MATERIALS AND METHODS:

2.1. Animals

Rhodnius prolixus were obtained from a laboratory colony maintained at 25–26°C and ~60% relative humidity in the Department of Physiology, University of Saskatchewan. Experiments were carried out at room temperature (20–23°C). Nymphal stages display the strongest diuresis, thus, I used fifth- and third-instar (nymphal stages) animals 1–4 weeks after molting.

Malpighian tubules were dissected from the animals under control saline (see below, Fig. 3) with the aid of a dissecting microscope. I used only the fluid-secreting distal tubule, which comprises the two-thirds (~25 mm) most distant segment of the tubule. The distal tubule is comprised of a single cell type whose secretory properties are uniform along its length and lacks contractile cells. The tubules are one cell thick and are made up of one or few cells encircling the lumen [13,46].

2.2. Saline solutions

Control saline resembles the hemolymph in osmolarity and composition. It contains (in mmol l^{-1}) 122.6 NaCl, 14.5 KCl, 8.5 $MgCl_2$, 2.0 $CaCl_2$, 10.2 $NaHCO_3$, 4.3 NaH_2PO_4, 8.6 HEPES and 20 glucose. Nominal Ca^{2+}-free saline contained (in mmol l^{-1}) 122.6 NaCl, 14.5 KCl, 8.5 $MgCl_2$, 10.2 $KHCO_3$, 4.3 KH_2PO_4, 8.6 HEPES and 20 glucose.. All saline solutions were at pH 7.

2.3. Secretion assays

Malpighian tubule distal fluid secretion rates were measured using a modified Ramsay assay as described previously [12]. Briefly, the distal segment of Malpighian tubules was isolated in a 90 µl droplet of bathing saline under paraffin oil. The cut end of the tubule was pulled out of the saline and wrapped around a fine steel pin pushed into the Sylgard base of a Petri dish (see Fig. 3). Finally, a nick was made in the section of the tubule immersed under paraffin oil, out of the droplet of bathing saline. Stimulation was achieved by the addition of 10 µl of serotonin (5-hydroxytryptamine, 100 µmol l^{-1}) into the bath droplet; leading to a final stimulus concentration

of 1 µmol l^{-1}. After stimulation with serotonin secreted droplets formed at the nick of the tubule and were pulled away every 5, 10 or 20 minutes using a fine glass probe (Fig. 3). The secreted droplets were photographed using a microscope digital camera (MiniVid, LW Scientific, Lawrenceville, GA, USA).

The droplets' diameters (d) were measured from the stored images using Image J 1.32 software (NIH, USA). The volume (*V*) of the secreted droplets was calculated using the formula for a sphere volume (see Equation 1), and secretion rate was calculated by dividing droplet volume by the time over which it formed.

$$V = \frac{4}{3}\pi r^3 \quad \text{..... (Equation 1)}$$

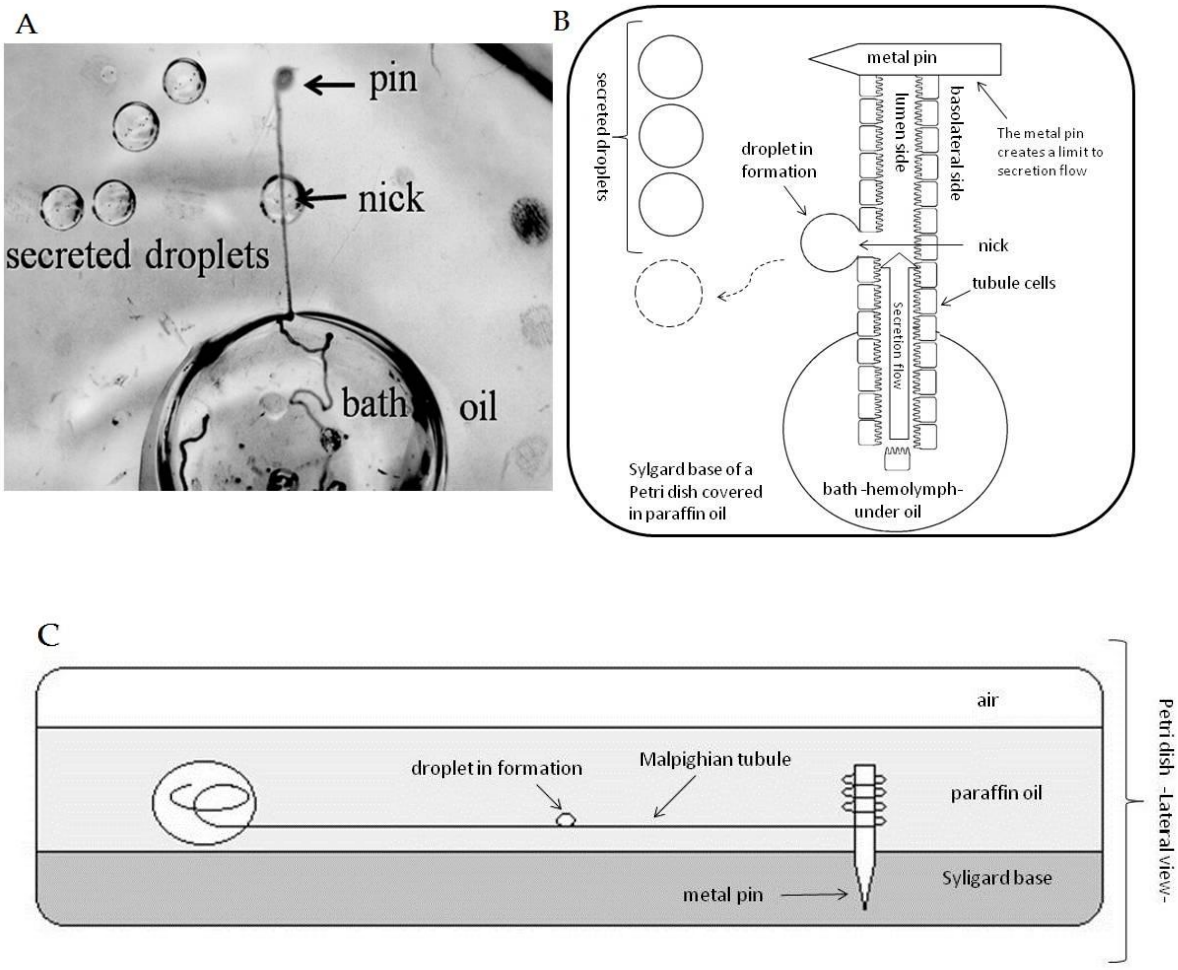

Figure 3: The Ramsay assay. The distal segments of Malpighian tubules are placed in a bath of saline solution under paraffin oil. A: Photograph of an experiment showing a Malpighian tubule set up for secretion assay. B: Cartoon explaining the image in panel A. C: Cartoon showing a lateral view of the preparation. The cut end of the tubule is wrapped around a steel pin and a nick is made in the segment under oil. After stimulation with 1 µmol l^{-1} serotonin in the bath, secreted droplets are produced at the nick and are pulled away every 5, 10 or 20 min. The volume of fluid produced by the tubule is calculated using the formula for a sphere.

2.4. Transepithelial potential measurement

The transepithelial potential (TEP) was measured using the Ramsay technique [20,47]. The secretory (distal) segment of a Malpighian tubule from a fifth-instar insect was isolated in a 100 µl droplet of bathing saline under paraffin oil. The cut end of the tubule was pulled out and wrapped around a pin, a nick was made in the segment of the tubule outside of the bathing droplet. A voltage-sensing electrode was placed in the nick in direct contact with the lumen of the tubule. A reference electrode was placed in the bathing droplet (see Figure 3). The distance between the sensing electrode and the bathing saline electrode was 2-3 mm. After positioning of the electrodes, the Malpighian tubule was stimulated with 1 µmol l^{-1} serotonin. Both electrodes were filled with 1 mol l^{-1} KCl and connected to a high impedance amplifier (FD223A, World Precision Instruments, Sarasota, FL, USA) and a PC data acquisition system (Labchart 7pro V.7.2.1, Powerlab 4/35, ADintruments, Sydney, Australia). All TEPs were measured inside a Faraday cage.

2.5. Measurement of K^+, Na^+ and pH in secreted droplets

Distal tubules from fifth-instar insects were isolated and set up in a secretion assay as described above, subsequently secreted droplets were collected. The pH, Na^+ and K^+ concentration in the secreted droplets were measured using ion-selective microelectrodes as described previously [21,48,49].

pH was measured immediately after collection of the droplets to avoid changes in the pH due to equilibration with atmospheric CO_2.

H^+, K^+ and Na^+-selective microelectrodes were produced as described before [12]. In short, borosilicate capillaries (World Precision Instruments, Sarasota, USA) were pulled using a vertical micropipette puller (PE-2, Narishige, Japan). The electrodes were silanized with dichlorodimethylsilane (Sigma, St. Lois, MO, USA) and baked for 20 minutes at 250ºC. Na^+-selective electrodes were based on sodium ionophore I, cocktail A (Fluka, Sigma, St. Lois, MO, USA) and backfilled with 0.5 mol l^{-1} NaCl. Sodium ionophore I, cocktail A contains 10% sodium ionophore I, 89.5% 2-nitrophenyl octyl ether and 0.5% sodium tetraphenylborate. The reference electrode was backfilled with 1 mol l^{-1} KCl^-. Na^+-selective electrodes were calibrated in solutions of (in mmol l^{-1}) 15 NaCl:135 KCl and 150 NaCl.

K^+-selective electrodes were based on potassium ionophore I, cocktail B (Fluka, Sigma, St. Lois, MO, USA) and backfilled with 1 mol l^{-1} KCl. Potassium ionophore I cocktail B contains 5% potassium ionophore I, 25% 1,2-dimethyl-3-nitrobenzene, 68% dibutyl sebacate and 2% potassium tetrakis (4-chlorophenyl)borate. The reference electrode was filled at the tip with 1 mol l^{-1} Na^+ acetate and the rest with 1 mol l^{-1} KCl^-. K^+-selective electrodes were calibrated in solutions of (in mmol l^{-1}) 15 KCl:135 NaCl and 150 KCl.

H^+-selective microelectrodes were based on hydrogen ionophore I, cocktail B (Fluka, Sigma, St. Lois, MO, USA). The H^+-selective electrodes were backfilled with 0.1 mol·l^{-1} sodium citrate + 0.1 mol l^{-1} NaCl. The reference barrel was filled with 1 mol l^{-1} KCl. Hydrogen ionophore I cocktail B contains 10% hydrogen ionophore I, 89.3% 2-nitrophenyl octyl ether, 0.7 % potassium tetrakis (4-chlorophenyl)borate. The H^+-selective electrode was calibrated in Ringer solutions at pH 7 and 6.

Only electrodes that displayed a change of ≥50 mV per 10 fold change in ion concentration of the calibration solution were used. Based on the Nernst equation an ideal

electrode would display a change of 59 mV per 10 fold change in concentration. During measurements, both the reference electrode and the ion sensing electrode were placed in each droplet under paraffin oil. The electrodes were connected through a high impedance amplifier (FD223A, World Precision Instruments, Sarasota, USA) to a PC data acquisition system (Labchart 7pro V.7.2.1, Powerlab 4/35, ADintruments, Sydney, Australia). All measurements were done inside a Faraday cage.

Ion concentration in secreted droplets was calculated using the formula:

$$c^d = c^c * 10^{\Delta V/s} \quad \text{(Equation 2)}$$

where c^d is the ion concentration in the secreted droplet, c^c is the ion concentration in one of the calibration solutions, ΔV is the difference in voltage measured between the secreted droplet and the same calibration solution, and S is the slope of the electrode (i.e. mV change in response to a 10-fold change in ion concentration in the calibration solutions).

Although ion-selective microelectrodes measure ion activity and not concentration, data can be expressed in terms of concentrations if it is assumed that the ion activity coefficient is the same in calibration and experimental solutions [46]. Ion flux ($nmol \cdot min^{-1}$) was calculated as the product of secretion rate ($nl \cdot min^{-1}$) and ion concentration ($mmol \cdot l^{-1}$) in the secreted droplets.

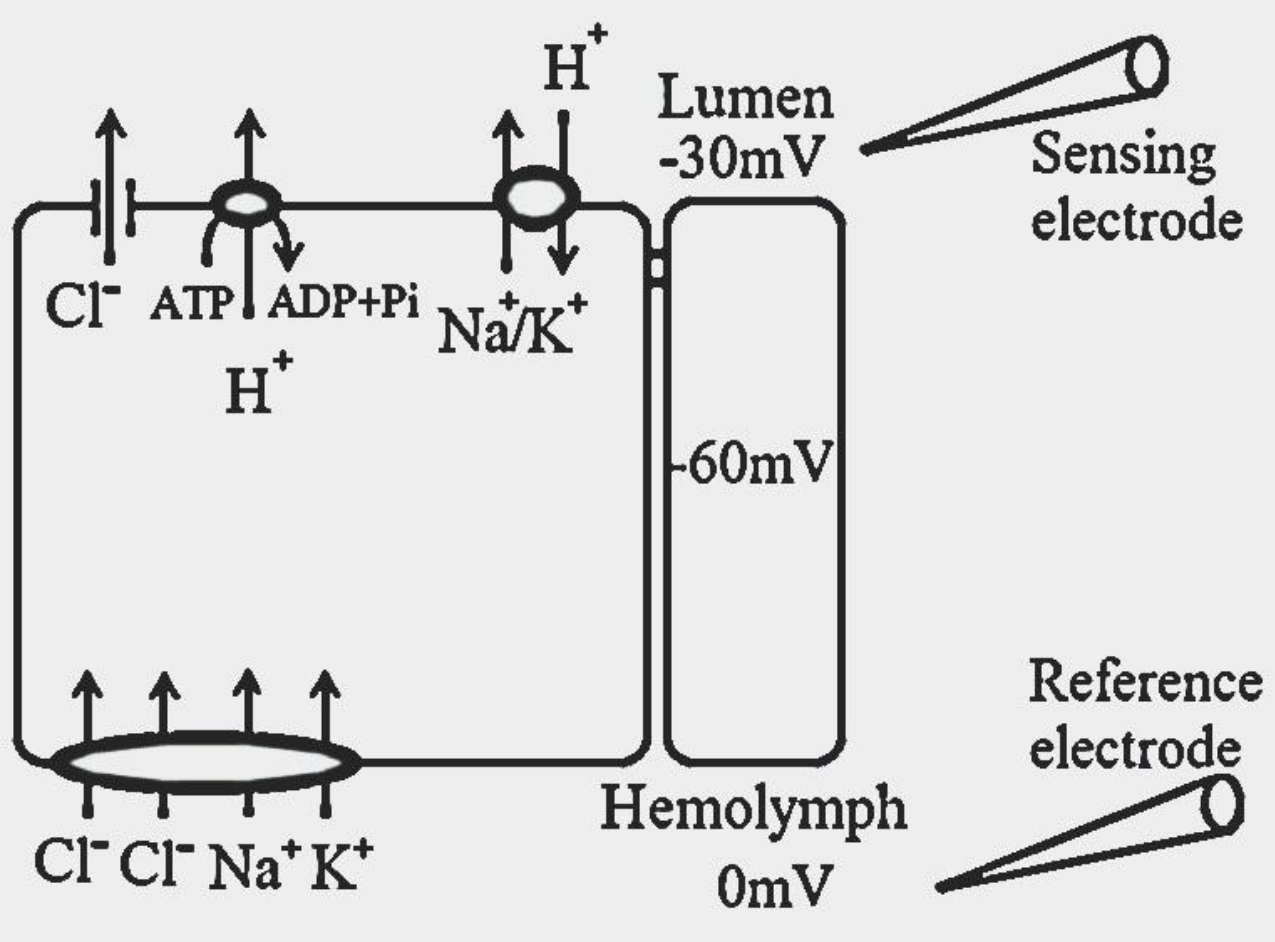

Figure 4: Transepithelial potential. The reference electrode is placed in the bath and the sensing electrode in small droplet of fluid collected at the nick in contact with the lumen of the tubule. Both electrodes are filled with 1 mol l^{-1} KCl and connected to a high impedance amplifier.

2.6. Calcium imaging

Distal Malpighian tubules from third-instar insects were isolated and placed in a custom built chamber with a glass bottom. The chamber was treated with poly-L-lysine to facilitate adhesion of the tubule to the bottom of the chamber (Sigma, St. Lois, MO, USA). The tubules were incubated at room temperature in the dark for 60 min in control saline containing 5 μmol l^{-1} Fura-2 AM, 1 mmol l^{-1} probenecid, and (0.1%) pluronic F-127. Probenecid, a drug known to block organic acid transport systems [50,51], was necessary to avoid Fura-2 extrusion from the cell.

After incubation, the Fura-2 AM solution was washed out with control saline solution. F-127 is non-ionic surfactant and it helps AM esters to disperse better. Probenecid (1 mmol l^{-1}) was present in the preparation for the duration of the experiment. Calcium was visualized with an upright fluorescent microscope (BX61WI, Olympus, Tokyo, Japan). The light source for excitation was an arc lamp (Prior Lumen 200PRO, Prior Scientific, Inc. Cambridge, UK) that was filtered with 340 nm or 380 nm excitation filters on a filter wheel (BrightLine, Semrock, Inc. Rochester, NY, USA). Measurements were collected every 0.5-1 sec with each excitation wavelength with an EMCCD camera (QImaging Rolera EM-C2, QImaging designs, Surrey, BC, Canada) after being filtered with a 510 nm emission filter (BrightLine, Semrock, Inc. Rochester, NY, USA). The intensity ratios after 340nm/380nm excitation were calculated using the software Metafluor Version7.0 (Molecular Devices, California, USA). A 20X water immersion optical lens was used to visualize the Malpighian tubules. Primary amplitude of ratiometric measurements was calculated from the baseline to the peak of each oscillation and frequency from peak to peak.

2.7. Reagents

Fura-2 AM and pluronic F-127 were obtained from Life Technologies Inc. (Burlington, Ontario, Canada). Stock solutions of Fura-2 AM and pluronic F-127 were prepared in anhydrous dimethyl sulfoxide (DMSO). The maximal final concentration of DMSO was <1% (v/v). Previous studies have shown that Malpighian tubule secretion rate is unaffected by DMSO at concentrations <1% (v/v) [20]. Malpighian tubules were exposed to different pharmacological drugs, 5µmol l^{-1} xestospongin C [52] (Tocris, Bioscience, Bristol, UK), 5µmol l^{-1} chelerythrine chloride [53] (Tocris, Bioscience, Bristol, UK), 30 or 300µmol l^{-1} BAPTA-AM [51] (Tocris, Bioscience, Bristol, UK), 10µmol l^{-1} bisindolylmaleimide-I [54] (Sigma, St. Louis, MO, USA), 1 mmol l^{-1} 8-Bromoadenosine-3',5'-cyclic monophosphate sodium salt (8Br-cAMP)[18] (Sigma, St. Louis, MO, USA) and 1 µmol l^{-1} bumetanide [21] (Tocris, Bioscience, Bristol, UK).

2.8. Statistics

Data are presented as mean ± SEM and analyzed using ANOVA or Student's t-test as appropriate. The analyses were carried out using GraphPad Prism 5 (GraphPad Software, Inc. La Jolla, CA, USA).

3. RESULTS:

3.1. Serotonin triggers intracellular Ca^{2+} oscillations (Figures 5-10):

Serotonin is a natural diuretic hormone in *R. prolixus*, this hormone is release into the hemolymph by the abdominal nerves. Only after 60 minutes after the onset of feeding serotonin levels decrease [55].

Stimulation with serotonin (1 µmol l^{-1}) triggered fluid secretion in Malpighian tubules bathed in control saline or Ca^{2+}-free saline containing the extracellular Ca^{2+} chelator EGTA (1 mmol l^{-1}, Fig. 5A). These results are consistent with previous reports that Ca^{2+}-free extracellular environment has no effect on serotonin-stimulated fluid secretion [28]. However, incubation of Malpighian tubules in Ca^{2+}-free saline containing the intracellular Ca^{2+} chelator BAPTA-AM significantly reduced serotonin-stimulated secretion by 75% (Fig. 5A, $p<0.05$, n=18 tubules for control, EGTA and BAPTA-AM groups, repeated measures two way ANOVA, Tukey-Kramer multiple comparison test). BAPTA-AM is highly selective for Ca^{2+} over Mg^{2+} and its binding capacities are not significantly altered by pH. BAPTA-AM is cell permeable thanks to the AM form, an ester groups that make the molecule uncharged. After BAPTA-AM crosses the membranes the AM group is cleaved by internal esterases. Secretion rate recovered in tubules where BAPTA-AM was washed away for 1h, suggesting that BAPTA-AM does not have a toxic effect (Fig. 5B, $p<0.05$, n=8 tubules for control, n=12 for BAPTA-AM groups, two-way repeated-measures ANOVA, Tukey-Kramer multiple comparison test). It is likely that Malpighian tubule extrude BAPTA out of the cell through transport systems specialized in organic molecules.

The results suggested that stimulation with serotonin involves intracellular Ca^{2+}. Thus, it was decided to observe intracellular Ca^{2+} in the distal segment of Malpighian tubules using Fura-2 AM.

Serotonin (1 µmol l^{-1}) stimulation triggered intracellular Ca^{2+} oscillations (Fig. 6, upper panel, n=28). The response varied among cells; where most cells (70%) responded immediately after addition of serotonin (Figure 6, graph 1, bottom right panel), some (20%) responded later and a few (4%) never responded (Fig. 6, graph 6, bottom right panel). Moreover, not all cells responded with the same intensity (see bottom panel from selected regions 1 to 6). Finally, the Ca^{2+} signals seemed to propagate from one cell to another (Fig. 6, bottom left panel). It was noticed that final cells of the distal tubules, those in the blinded end, were always immediate responders.

Distal Malpighian tubule cells responded to serotonin with an initial increase in cytoplasmic Ca^{2+} followed by persistent Ca^{2+} waves that, in some cases, remained for the complete duration of the experiment (~10 min). The effect of serotonin on intracellular Ca^{2+} was completely blocked by pre-incubation of the tubules with Ca^{2+}-free saline containing BAPTA-AM (30 µmol l^{-1}, Fig. 7.

Incubation in Ca^{2+}-free saline containing 1 mmol l^{-1} EGTA did not block the intracellular Ca^{2+} waves triggered by serotonin (Fig. 7) but altered their frequency. EGTA-treated tubules produced Ca^{2+} oscillations upon serotonin stimulation that were initially similar to control tubules but after a few minutes of stimulation, the Ca^{2+} waves in control experiments show a lower frequency than EGTA-treated tubules (Fig. 9). If Ca^{2+} is hypothesized to play a role in the modulation of ion transporters, the difference found in Ca^{2+} frequencies (in EGTA-treated tubules) may indicate that the transport properties of the tubule are altered. Thus, I measured the

rate and ion (Na^+ and K^+) concentrations of serotonin-stimulated tubules secretion treated with EGTA. EGTA-treated tubules showed no differences in ion concentration (Fig. 10) or secretion rate (Fig. 5) compared to controls. The results suggest that EGTA doesn`t affect the secretory response in serotonin-stimulated distal tubules of *R. prolixus*. In contrast, treatment with BAPTA-AM blocks intracellular Ca^{2+} waves and reduces serotonin-stimulated secretion rate by 75% (Fig. 5A). This is the first demonstration of a role for Ca^{2+} in serotonin-stimulated fluid secretion in *R. prolixus* Malpighian tubules.

3.2. Ca^{2+} affects the bumetanide-sensitive Na^+:K^+:2Cl^- cotransporter in serotonin stimulated tubules (Figure 11-13):

To test the role of intracellular Ca^{2+} on ion transporters I measured the transepithelial potential (TEP). Stimulation with serotonin triggers a characteristic shift in the TEP; that has three phases (Fig. 11A). Each of the phases is driven by the activation of a particular ion transport system. During the first phase, activation of apical Cl^- channels drive the TEP to more negative voltages. Phase two consists of a rapid deflection of the TEP to positive potential. This phase results from the activation of apical V-type H^+-ATPase. The third phase drives the TEP back to negative potential. This last phase is dependent on the activation of basolateral bumetanide-sensitive NKCC cotransporter that increases intracellular Cl^- concentration and, thus, the driving force for Cl^- movement through apical Cl^- channels [20] (Fig. 3).

Stimulation with serotonin triggered the characteristic triphasic voltage response in tubules incubated in control saline (labeled phase 1, 2 and 3 in Fig. 11 A) [20]. Similarly, tubules incubated in Ca^{2+}-free saline plus EGTA triggered a triphasic response indistinguishable from control experiments (Fig. 11 A and B). In contrast, tubules incubated in Ca^{2+}-free saline plus

BAPTA-AM failed to trigger the 3rd phase (Fig. 11 A and B). Phase 3 in tubules treated with BAPTA-AM is significantly different to control and EGTA treated tubules (Fig. 11 C). The results suggest that chelating intracellular Ca^{2+} with BAPTA-AM has no effect on apical Cl^- channels and V-type H^+-ATPase. However, it seems to inhibit basolateral NKCC.

To further test the role of Ca^{2+} on the modulation of the activity of the basolateral NKCC cotransporter I measured pH and ion composition of the secreted fluid. The results show that both the pH and ion composition of the secreted fluid are altered in tubules incubated in Ca^{2+}-free saline plus BAPTA-AM. The secreted fluid pH decreased from 7.1 ± 0.01 to 6.2 ± 0.06 in tubules incubated in control saline and Ca^{2+}-free saline plus BAPTA-AM, respectively (Fig. 12, $p<0.05$, n=10 for both groups, Student's t-test). The effect of Ca^{2+} depletion on luminal pH could be explained by a slower Na^+ and K^+ entry across the basolateral NKCC cotransporter that would reduce the availability of Na^+ and K^+ for exchange with luminal H^+ via apical Na^+ or K^+/H^+ exchanger(s) [20]. An alternative hypothesis is that Ca^{2+} directly affects the apical Na/H^+ exchanger, leading to a more acidic pH. Both hypotheses need to be tested.

The results also show that concentration and flux of Na^+ significantly decreased when tubules were incubated in Ca^{2+}-free saline plus BAPTA-AM (Fig. 13 A and B, $p<0.05$, n=14 for BAPTA-AM and 21 for control, repeated measures ANOVA, Tukey-Kramer multiple comparison test). In contrast, K^+ concentration significantly increased in the secreted fluid when tubules were incubated in Ca^{2+}-free saline plus BAPTA-AM (Fig. 13 C, $p<0.05$, n=52, repeated measures ANOVA, Tukey-Kramer multiple comparison test). Even though the concentration of K^+ increased in tubules incubated in Ca^{2+}-free saline plus BAPTA-AM, the K^+ flux decreased (Fig. 13 D, $p<0.05$, n=52, repeated measures ANOVA, Tukey-Kramer multiple comparison test). When comparing ion fluxes it can be observed that the reduction in Na^+ flux doubles that of K^+.

This may be explained by the contribution of Na^+-K^+ATPase that drives K^+ into the cells. Thus, blockage of K^+ entry though the NKCC may be partially restored by K^+ flux though the Na^+-K^+ATPase. In contrast, there is no alternative Na^+ pathway when blocking NKCC. Thus, blocking NKCC has a relatively larger effect on Na^+ than K^+ flux. Similar results were reported in tubules treated with the NKCC cotransporter, bumetanide [12]. Thus, taken together, the results seem to suggest that Ca^{2+} is required for normal activation of the basolateral NKCC cotransporter.

3.3. Ca^{2+} signaling is cAMP-mediated (Fig. 14-16)

Serotonin has been shown to stimulate cAMP production in the tubules and addition of cAMP produces full secretion [56]. Thus, I tested the relationship between cAMP and Ca^{2+} signaling. Stimulation with the membrane permeable cAMP analogue 8Br-cAMP 1mmol l^{-1} showed no differences in secretion rates when compared to tubules stimulated with serotonin. Furthermore, Ca^{2+} chelation with 300 µmol l^{-1} BAPTA-AM decreased 8Br-cAMP-stimulated secretion rate by 40% from 48±2 to 31±2 nl min^{-1} (Fig. 14, $p<0.05$, n=19 for serotonin controls, n= 17 for 8Br-cAMP and n=22 for 8Br-cAMP plus BAPTA-AM, repeated measures ANOVA, Tukey-Kramer multiple comparison test). 8Br-cAMP triggered Ca^{2+} waves with similar amplitude but higher frequency than those produce by serotonin controls (Fig. 15 B, $p>0.05$, n=8 for 8Br-cAMP and n=13 for serotonin control, repeated measures ANOVA, Tukey-Kramer multiple comparison test). The secretion rate, K^+ and Na^+ composition was not changed in 8Br-cAMP-stimulated tubules when compare to serotonin controls (Fig.16, $p>0.05$, Na^+: n=5 for 8Br-cAMP, n=7 for serotonin control group. K^+: n=10 for cAMP, n=10 for serotonin, repeated measures two way ANOVA, Tukey-Kramer multiple comparison test). 8Br-cAMP stimulated

tubules incubated in BAPTA-AM showed an increase in K^+ concentration and a decrease in Na^+ concentration in the secreted droplets (Fig. 16 A and C, $p<0.05$). The same trend was observed in serotonin-stimulated tubules incubated with BAPTA-AM (Fig. 10), suggesting 8Br-cAMP and serotonin may trigger the same intracellular Ca^{2+} signaling pathway. However, it is interesting to point out that BAPTA-AM decreases only 40% the secretion rate and not 75% as in serotonin stimulated tubules. This inconsistency could be explained by two reasons; (I) the concentration used of 8Br-cAMP may not be similar to physiological cAMP production. (II) 8Br-cAMP is a non-hydrolyzable analog of cAMP, therefore the cAMP phosphodiesterase can not break it down, affecting regulatory mechanisms and the internal concentration of cAMP.

Na^+ flux decreased when 8Br-cAMP stimulated tubules were incubated with BAPTA-AM while K^+ flux didn't show significant differences (Fig. 16 B, $p<0.05$ and D, $p>0.05$, Na^+: n=5 for 8Br-cAMP, n=7 for serotonin and n=11 for BAPTA-AM. K^+: n=10 for cAMP, n=10 for serotonin group and n=11 for BAPTA-AM group, repeated measures two way ANOVA, Tukey-Kramer multiple comparison test). Taken together, the data suggest that 8Br-cAMP stimulates a maximal secretory response, similar to that induced by serotonin; that increases intracellular Ca^{2+} which subsequently up-regulates NKCC. Thus, the results indicate that cAMP must act upstream of Ca^{2+}.

3.4. PLC-PKC pathway is involved in serotonin-stimulated secretion (Figure 17-19).

Calcium dependent secretion described in other insects involves PLC and Ins3P [36] and in many other systems cAMP-PKA is coupled with PLC and PKC activation [57–60]. Therefore, I tested the role of PKC on serotonin-stimulated secretion in *R. prolixus*.

I used two PKC blockers which were reported to work successfully in Malpighian tubules, chelerythrine and BIM [54,61,62]. Chelerythrine doesn't inhibit tyrosine kinases, PKA or

calcium/calmodulin-dependent protein kinase. However there are some unspecific effects chelerythrine since it can activate p38 kinase and JUNK, inducing apoptosis in cancer cell lines. BIM is highly selective for all isoforms of PKC; it acts as a competitive inhibitor for the ATP binding site.

Treatment with chelerythrine decreased secretion from 51 ± 2 nl min^{-1} to 20 ± 3 nl min^{-1} (Fig. 17 A, $p<0.001$, n=15 for serotonin control group, n=15 for 5 µmol l^{-1} chelerythrine treated group, repeated measures two way ANOVA, Tukey-Kramer multiple comparison test). BIM-treated tubules decreased secretion rate by 50% from 40 ± 2 nl min^{-1} to 19 ± 1 nl min^{-1} (Fig. 17 B, $p<0.001$, n=24 for serotonin control group, n=25 for 10 µmol l^{-1} BIM treated group, repeated measures two way ANOVA, Tukey-Kramer multiple comparison test). The evidence suggests that PKC pathway is involved in serotonin stimulated secretion.

To further analyze the effect of PKC, I measured the effect of blockers on Na^+ and K^+ composition of the secreted fluid (Fig. 18). No significant differences were found between the controls and BIM-treated tubules in Na^+ and K^+ concentrations (Fig. 18 A and C, $p>0.05$). However both Na^+ and K^+ flux significantly decreased (Fig. 18 B and D, $p<0.001$ for Na^+ and $p<0.05$ for K^+) in BIM-treated tubules (Fig.18 Na^+: n=13 for control group, n=13 for BIM treated group. K^+: n=12 for control group, n=12 for BIM treated group, repeated measures two way ANOVA, Tukey-Kramer multiple comparison test). The flux results resemble those of BAPTA-AM treated tubules, where Na^+ flux decreased double compared to K^+ flux. The results suggest that PKC pathway is involved in secretion and blocking it affects the transport of ions. Based on the discussed above, PKC may be affecting the Na^+/H^+ exchanger or the NKCC.

An indirect way of testing the PLC activity is to test the role of InsP3 receptors (InsP3R). For that purpose, I used the highly selective blocker for InsP3R, xestospongin [52] (Fig. 19).

However, in vertebrate synapses, xestospongin caused a transient calcium elevation by inhibition of the sarcoplasmic/endoplasmic reticulum Ca^{2+} ATPase (SERCA) pump of internal stores. That effect was not observed in this study. Serotonin-stimulated tubules treated with 5 µmol l^{-1} xestospongin showed a slight decrease in secretion rate (Fig. 19 A, $p<0.05$, n=6 for control group, n=8 for xestospongin treated group, repeated measures two way ANOVA, Tukey-Kramer multiple comparison test). Xestospongin treatment significantly decreased the amplitude of serotonin-triggered Ca^{2+} waves (Fig. 19 B, $p>0.05$, n=13 for control group, n=4 for xestospongin treated group, repeated measures two way ANOVA, Tukey-Kramer multiple comparison test). The frequency was also affected (Fig 19 C, $p>0.05$, n=4 for xestospongin and n=13 for control, repeated measures ANOVA, Tukey-Kramer multiple comparison test). The results obtained from these experiments suggest that InsP3Rs may contribute to the Ca^{2+} waves and, thus, that PLC is active in serotonin-stimulated tubules. However, the failure of xestospongin to completely abrogate Ca^{2+} waves may suggest an alternative intracellular Ca^{2+} gate.

3.5. Ca^{2+} regulation feedback loop (Figure 20):

One of the main reasons for starting this research was the gap of knowledge about crosstalk between the apical and basolateral membranes of secretory epithelia. The function of channels, pumps and transporters located both at the apical and basolateral membranes have to be tightly coordinated to maintain intracellular ion homeostasis due to the massive ion transport rate displayed by *R. prolixus* tubules. For this reason, it is highly likely that the fine regulation of ion transporters/channels activity is far more complex than an "ON-OFF" model. A review of the literature suggests that Ca^{2+} may play a role as a modulator of the activity of the different ion transport systems [32,63]. In order to test the role of Ca^{2+} in the crosstalk between basolateral and

apical membrane, I studied how variations in intracellular ion concentration affected Ca^{2+} oscillations. A previous study has shown that blocking the basolateral NKCC after serotonin stimulation of the Malpighian tubules caused a large decrease of intracellular Cl^- [12]. Thus, I tested the effect of 1 µmol l^{-1} bumetanide, NKCC blocker, after the onset serotonin-stimulated Ca^{2+} waves. To test the effect of bumetanide I first waited for the oscillations to stabilize from the first Ca^{2+} burst (from 5 to 15 minutes) and only then added the drug. Treatment with bumetanide blocked the intracellular Ca^{2+} waves (Fig. 20, n=19). From these results I propose the working hypothesis that the Malpighian tubules cells are able to detect changes in intracellular Cl^- and modulate Ca^{2+} waves thus, altering ion transport. Based on our previous results, it seems feasible that Ca^{2+} triggers NKCC activation and that there is an ion sensor regulating a feedback loop from NKCC to Ca^{2+} stores.

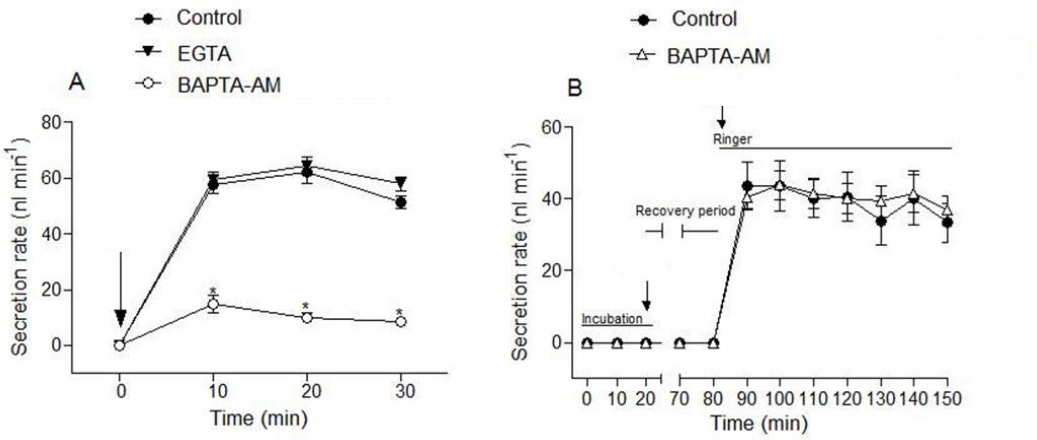

Figure 5: Secretion rate is reduced in BAPTA-AM treated tubules. A: Treatment with BAPTA-AM significantly reduced fluid secretion rate. MTs were bathed in control saline (filled circle), Ca^{2+}-free saline plus EGTA (1 mmol l^{-1}, filled triangle) or Ca^{2+}-free saline plus BAPTA-AM (300 µmol l^{-1}, open circle). Tubules were stimulated at time 0 with serotonin (1 µmol l^{-1}), marked with an arrow ($p<0.05$, n=18 for control, EGTA and BAPTA-AM, repeated measures two way ANOVA, Tukey-Kramer multiple comparison test). B: BAPTA-AM has no toxic effects on MTs. MTs were incubated in control saline (filled circles) or Ca^{2+}-free saline plus BAPTA-AM for 20 minutes (300 µmol l^{-1}, open triangle). After 20 minutes incubation tubules were stimulated with 1 µmol l^{-1} serotonin. After 10 extra minutes after serotonin stimulus, the tubules were transferred to fresh saline solution for 50 minutes to wash BAPTA-AM and serotonin. At time 80, tubules were transferred to new ringer solution in order to remove any BAPTA-AM traces and immediately stimulated with 1 µmol l^{-1} serotonin (marked with an arrow). Droplets were collected every 10 minutes from 90 to 150 minutes. BAPTA-AM treated MTs were able to recover secretion, no differences were found between this group and control tubules ($p>0.05$, n=8 for control, n=12 for BAPTA-AM recovery group, repeated measures two way ANOVA). Asterisks indicate significant difference. Bars represent SEM.

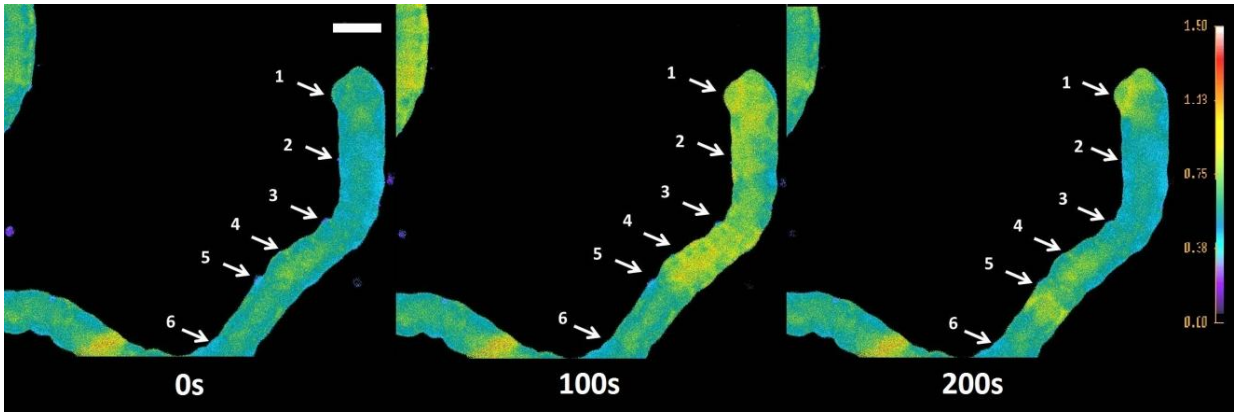

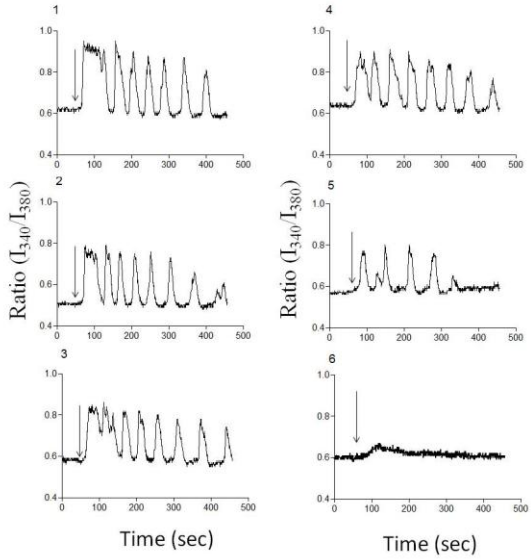

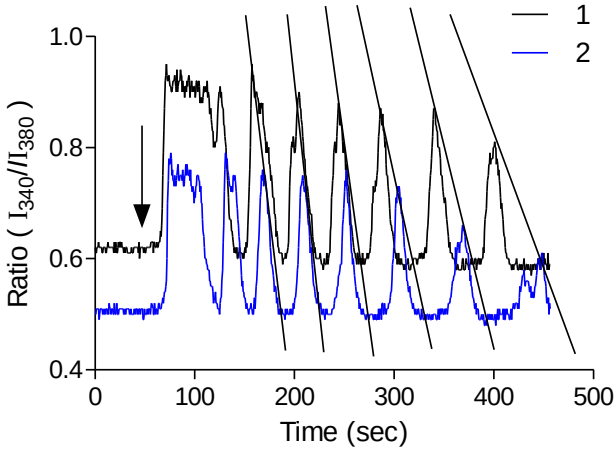

Figure 6: Serotonin stimulates Ca^{2+} waves. Tubules loaded with Fura2-AM in control saline were stimulated with 1 µmol l^{-1} serotonin. Upper panel: Shows the intensity ratio (I_{340}/I_{380}) at time 0 (when serotonin was added), 100 and 200 s after stimulation. I selected 6 regions of identical surface area, labelled 1 to 6, to measure the I_{340}/I_{380} ratio. The white scale bar represents 90 µm. Colour scale bar represents I_{340}/I_{380} ratio. Bottom right panel: The graphs labelled 1 to 6 show the I_{340}/I_{380} ratio over time of the areas selected in the upper panel. The addition of serotonin is marked with an arrow. Bottom left panel: regions 1 and 2 were overlapped to show the propagation effect between cells. To clarify the delay in the oscillations of the region 2, lines were used align the oscillation peaks of the two cells. This experiment was repeated 28 times with similar results.

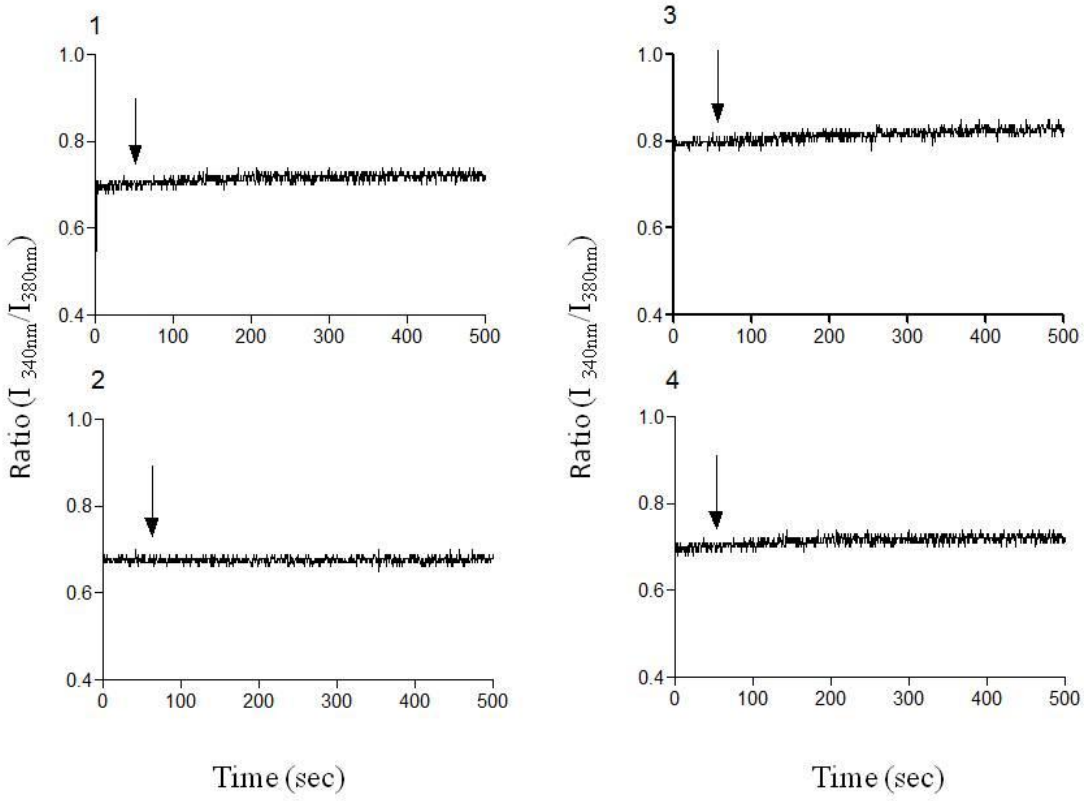

Figure 7: BAPTA-AM abrogates Ca^{2+} waves. Tubules loaded with Fura2-AM in Ca^{2+} free saline + 30 µmol l^{-1} BAPTA-AM were stimulated with 1 µmol l^{-1} serotonin (arrow). 4 regions of identical surface area were selected, labeled 1 to 4, and the I_{340}/I_{380} ratio analyzed. No Ca^{2+} oscillations were observed after serotonin stimulation. The graphs represent the ratio over time. This experiment was repeated 11 times with similar results.

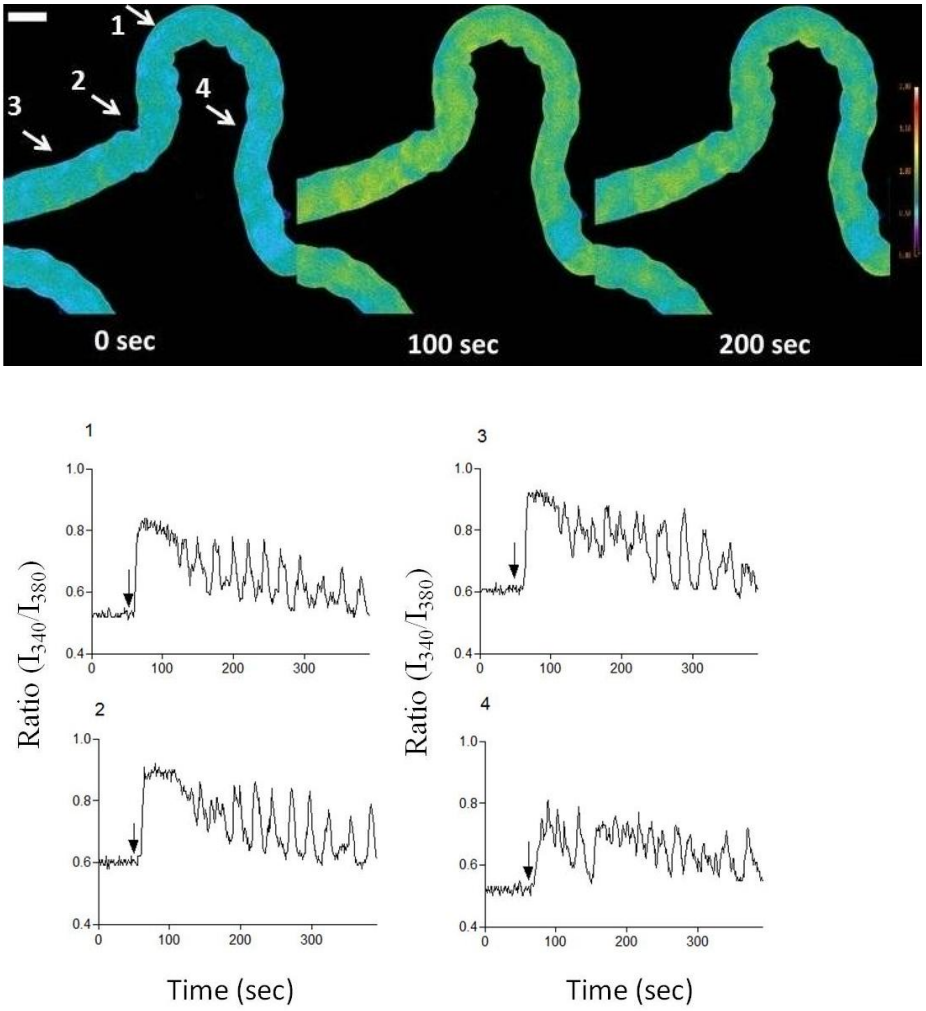

Figure 8: Serotonin-stimulated Ca^{2+} waves are not blocked by treatment with EGTA. Tubules loaded with Fura2-AM in Ca^{2+} free saline + 1 mmol l^{-1} EGTA were stimulated with 1 µmol l^{-1} serotonin. Upper panel: shows the I_{340}/I_{380} ratio after addition of serotonin at time 0 and the posterior 100 and 200s after stimulation. 4 regions of identical surface area were selected and I_{340}/I_{380} ratio analyzed. White scale bar represents 90 um. Color scale bar represents the I_{340}/I_{380} ratio. Bottom panel: The graphs labelled 1 to 4 show the I_{340}/I_{380} ratio over time of the areas selected in the upper panel. The addition of serotonin is marked with an arrow. EGTA doesn't block Ca^{2+} oscillations. This experiment was repeated 6 times with similar results.

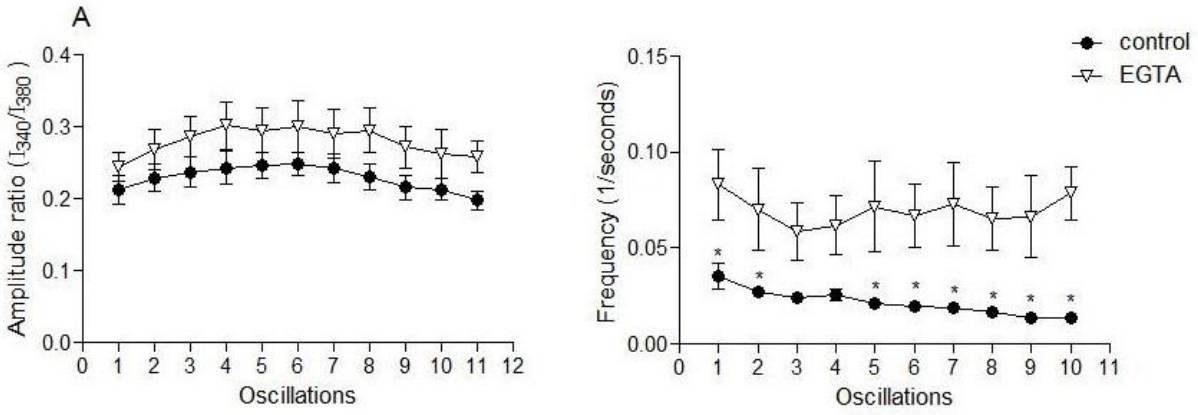

Figure 9: Oscillations and frequency of EGTA treated tubules. Tubules loaded with Fura2-AM in control saline or Ca^{2+} free saline + 1 mmol l^{-1} EGTA were stimulated with 1 µmol l^{-1} serotonin. The Ca^{2+} oscillations generated were analyzed. A: Amplitude of oscillations. There is no significant difference between control and EGTA groups. ($p>0.05$, control n=13, EGTA n=7 repeated measures two way ANOVA, Tukey-Kramer multiple comparison test). B: EGTA-treated tubules display Ca^{2+} waves that have a stable frequency in time while control group shows a decrease frequency over time (control n=13, EGTA n=7 repeated measures two way ANOVA, Tukey-Kramer multiple comparison test). Asterisks indicate significant difference. Bars represent SEM.

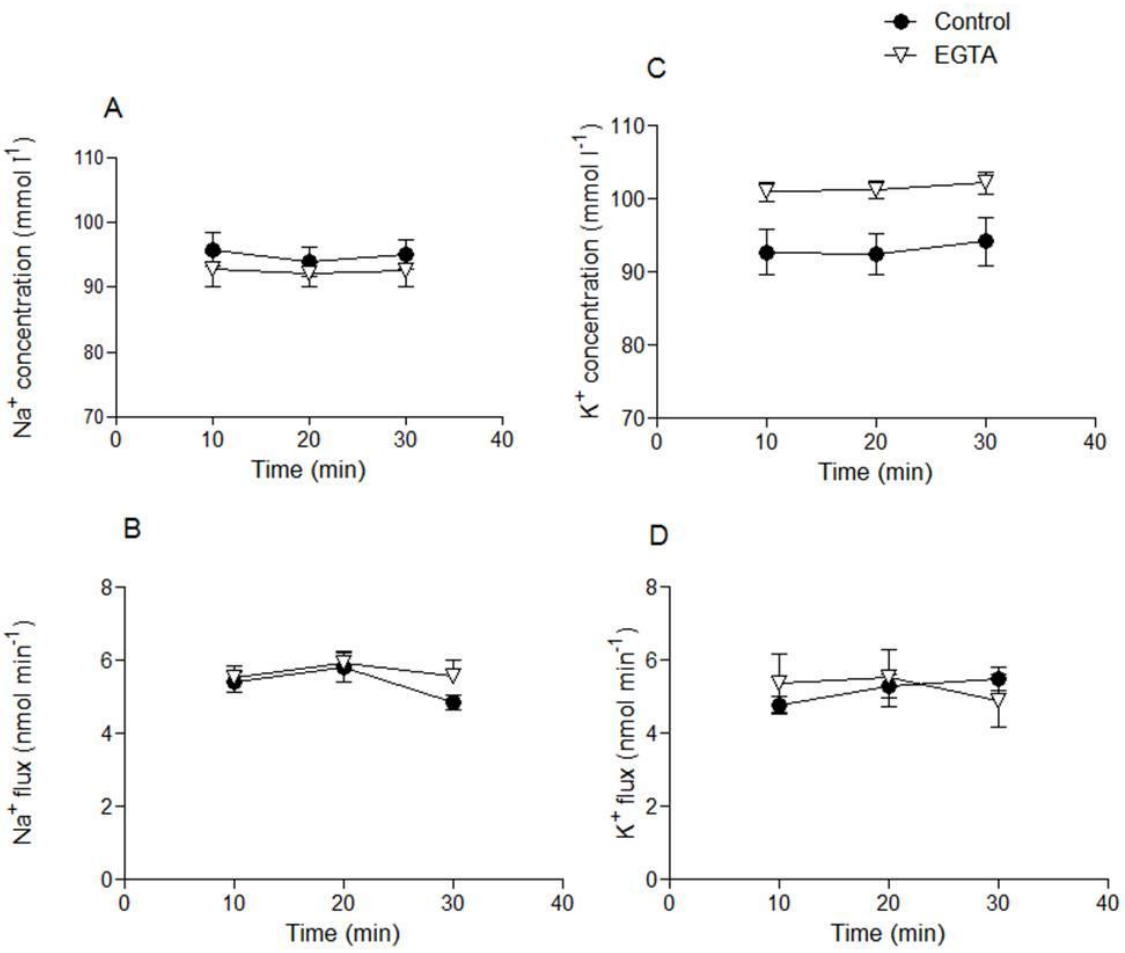

Figure 10: Na^+ and K^+ measurements of the secreted fluid in control and EGTA treated Malpighian tubules. Ions were measured after 1 µmol l^{-1} serotonin stimulation at time 0. Na^+ Concentration (A) and flux (B) in tubules incubated in Ca^{2+}-free saline plus 1 mmol l^{-1}EGTA don`t show significant differences compare to control ($p>0.05$, n=14 for control group and n=14 for $Ca^{2+}$-free saline plus EGTA group, repeated measures two way ANOVA, Tukey-Kramer multiple comparison test). $K^+$ concentration (C) and flux (D) don`t show differences between controls tubules and tubules incubated in Ca^{2+}-free saline plus 1 mmol l^{-1}EGTA ($p>0.05$, n=52 for control group and n=11 for EGTA, repeated measures two way ANOVA, Tukey-Kramer multiple comparison test). Bars represent SEM.

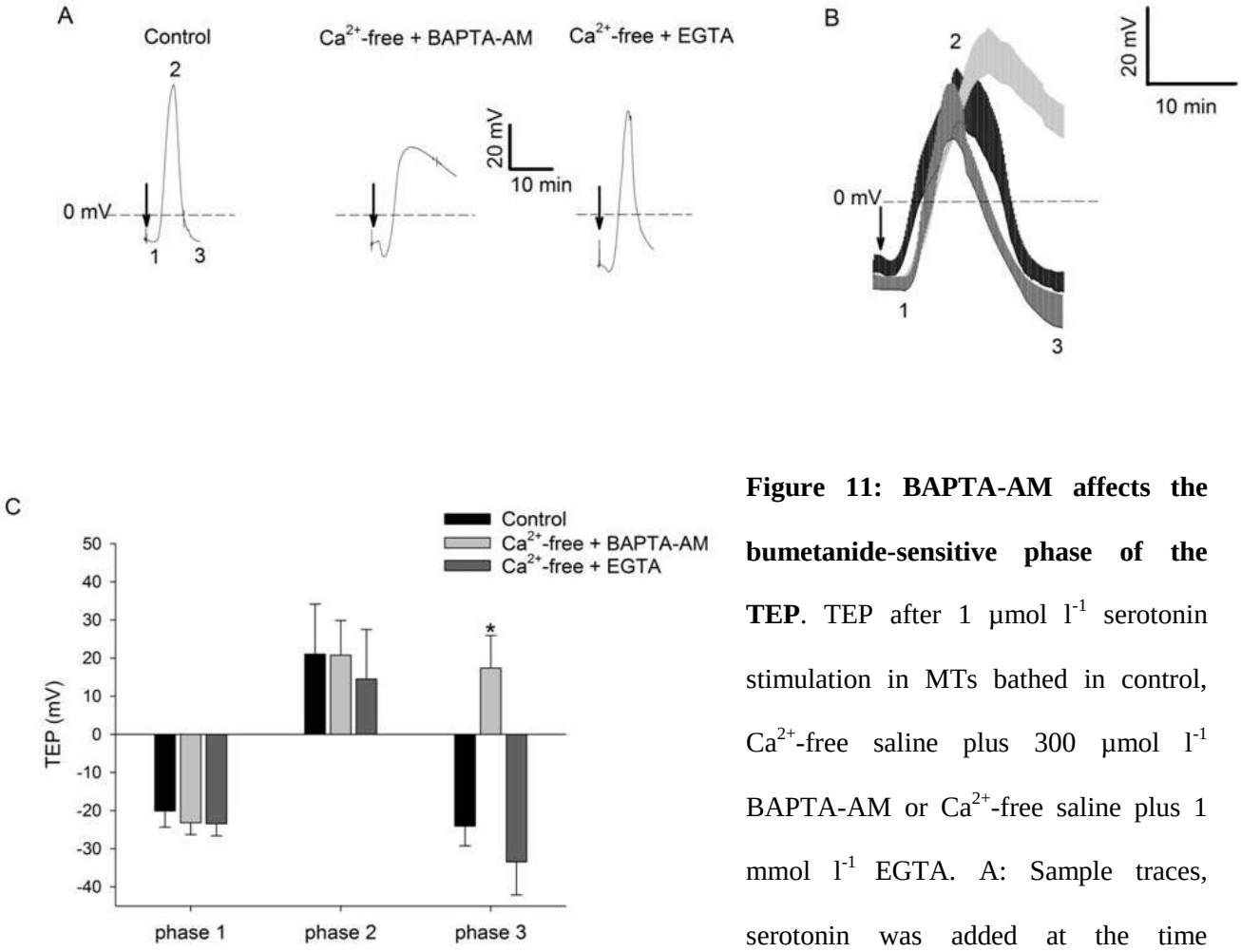

Figure 11: BAPTA-AM affects the bumetanide-sensitive phase of the TEP. TEP after 1 µmol l^{-1} serotonin stimulation in MTs bathed in control, Ca^{2+}-free saline plus 300 µmol l^{-1} BAPTA-AM or Ca^{2+}-free saline plus 1 mmol l^{-1} EGTA. A: Sample traces, serotonin was added at the time indicated by the arrow. B: Mean + SEM for tubules exposed to control, BAPTA-AM or EGTA treatments. The lower edge of each trace represents the mean and the upper edge represents the SEM. C: TEP value for phases 1, 2 and 3 of the triphasic response to serotonin. The TEP at the 3rd phase is significantly different for tubules incubated in Ca^{2+}-free saline plus BAPTA-AM ($p<0.05$, n=5 for control, n=7 for BAPTA-AM and n=5 for EGTA, ANOVA, Tukey-Kramer multiple comparison test, asterisks indicate significant difference).

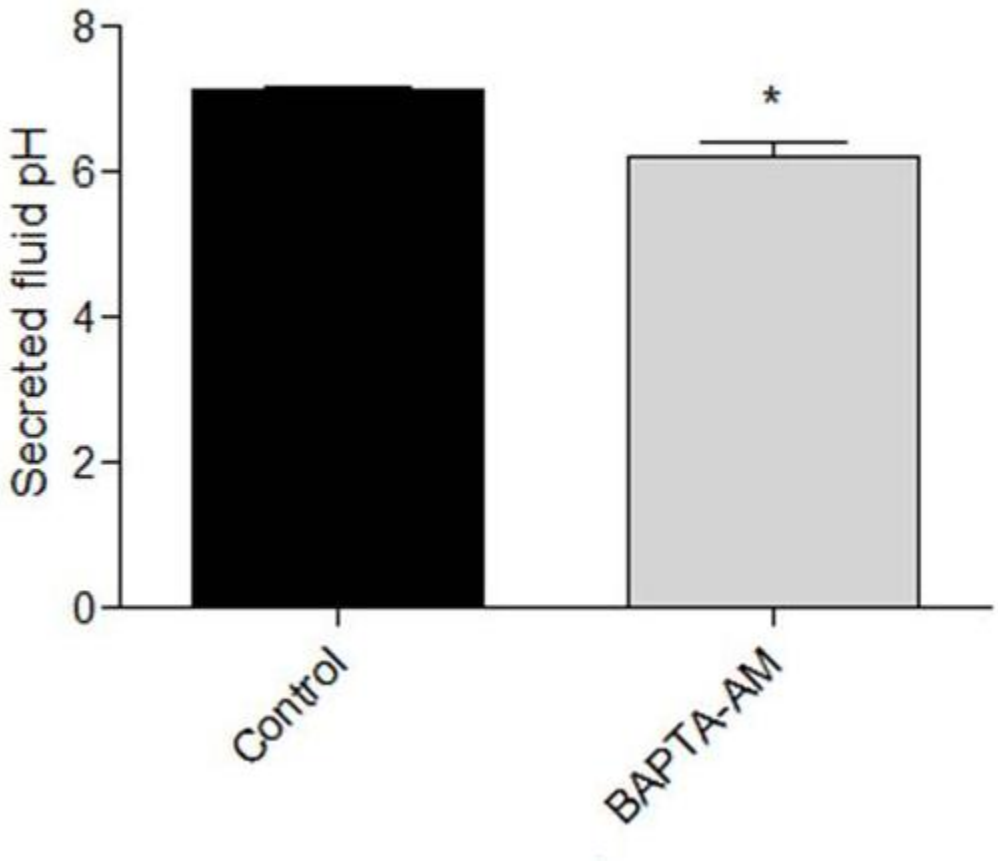

Figure 12: Effect of BAPTA-AM on the pH of the secreted fluid. pH was measured with ion selective electrodes. Incubation in Ca^{2+}-free saline containing 300 µmol l^{-1} BAPTA-AM caused a 1 unit decrease in pH of the fluid secreted after 1 µmol l^{-1} serotonin stimulation ($p<0.05$, n=10, Student's t-test, asterisks indicate significant difference).

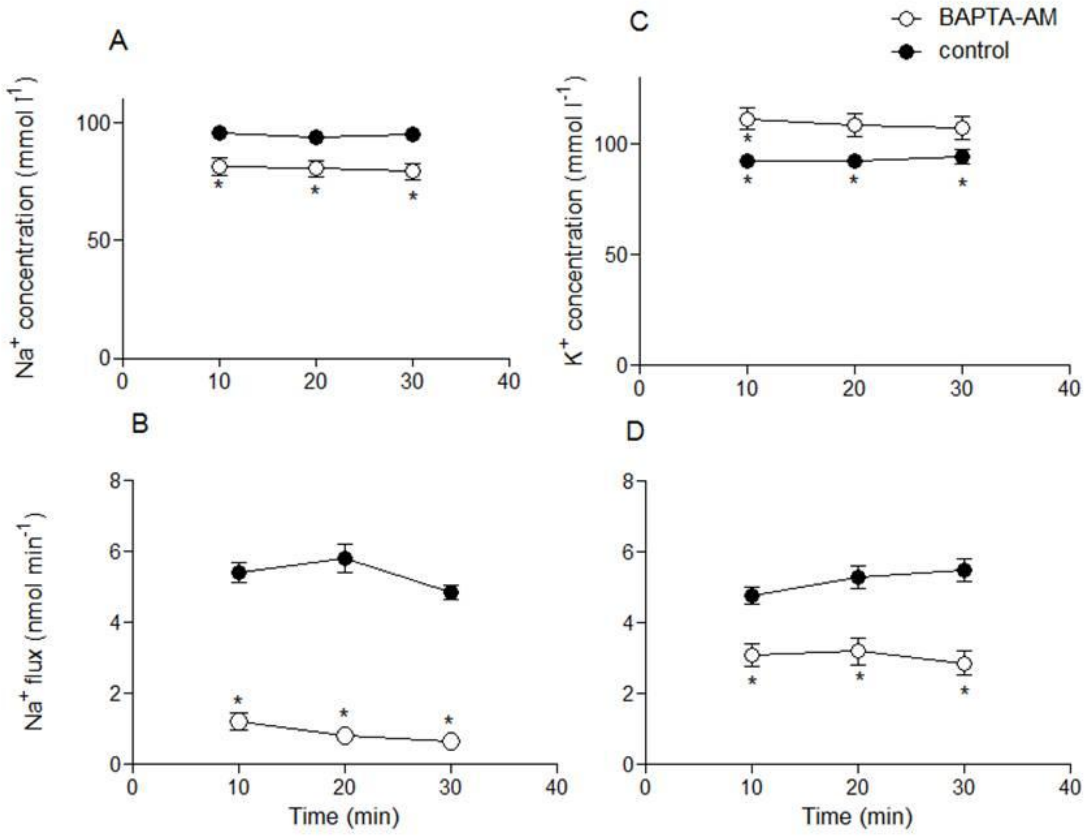

Figure 13: Ion composition of the secreted fluid is altered in BAPTA-AM treated tubules. Na^+ concentration (A) and flux (B) are significantly reduced in tubules incubated in Ca^{2+}-free saline plus 300 µmol l^{-1} BAPTA-AM ($p<0.05$, n=23 for controls and n=21 for BAPTA-AM group, repeated measures two way ANOVA, Tukey-Kramer multiple comparison test). K^+ concentration is increased (C) and flux is reduced (D) in tubules incubated in Ca^{2+}-free saline plus 300 µmol l^{-1}BAPTA-AM ($p<0.05$, n=52 for each group, repeated measures two way ANOVA, Tukey-Kramer multiple comparison test). Asterisks indicate significant difference. Bars represent SEM.

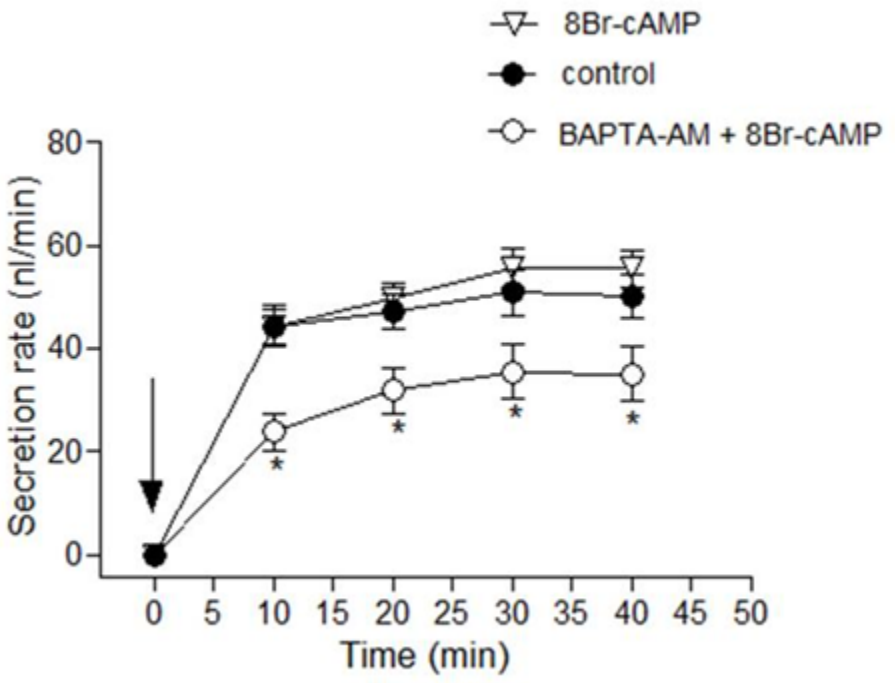

Figure 14: Secretion rate is decreased in BAPTA-AM-treated tubules stimulated with 8Br-cAMP. MTs bathed in control saline were stimulated with 1 µmol l^{-1} serotonin controls (filled circle) or 1 mmol l^{-1} 8Br-cAMP (open triangle) at time 0 (arrow). Treatment with 8Br-cAMP showed no significant differences compare with serotonin controls. Tubules incubated in Ca^{2+}-free saline plus 300 µmol l^{-1}BAPTA-AM stimulated with 8Br-cAMP (open circle) significantly reduced fluid secretion rate compare to both 8Br-cAMP and serotonin control tubules. ($p<0.05$, n=19 for serotonin controls, n= 17 for 8Br-cAMP and n=22 for 8Br-cAMP plus BAPTA-AM, repeated measures ANOVA, Tukey-Kramer multiple comparison test, asterisks indicate significant difference). Bars represent SEM.

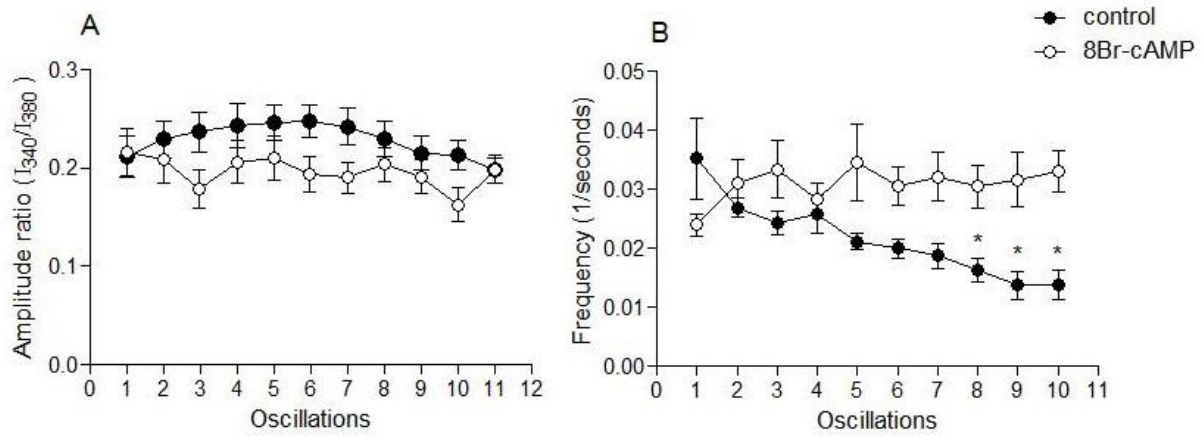

Figure 15: Analysis of Ca^{2+} oscillations in 8Br-cAMP stimulated tubules. Tubules loaded with Fura2-AM were stimulated with 1 µmol l^{-1} serotonin (control) or 1 mmol l^{-1} 8Br-cAMP. Both stimulus generated Ca^{2+} oscillations that were analyzed. A: Amplitude of Ca^{2+} oscillations. There is no significant difference between control and 8Br-cAMP groups ($p<0.05$, n=13 for control, n=8 for 8Br-cAMP, repeated measures two way ANOVA, Tukey-Kramer multiple comparison test) B: Frequency of Ca^{2+} oscillations. After 8Br-cAMP stimulation MTs showed a stable frequency while control group shows a decrease in frequency over time. The last three points show significant differences ($p<0.05$, n=8 for 8Br-cAMP and n=13 for control, repeated measures ANOVA, Tukey-Kramer multiple comparison test, asterisks indicate significant difference). Bars represent SEM.

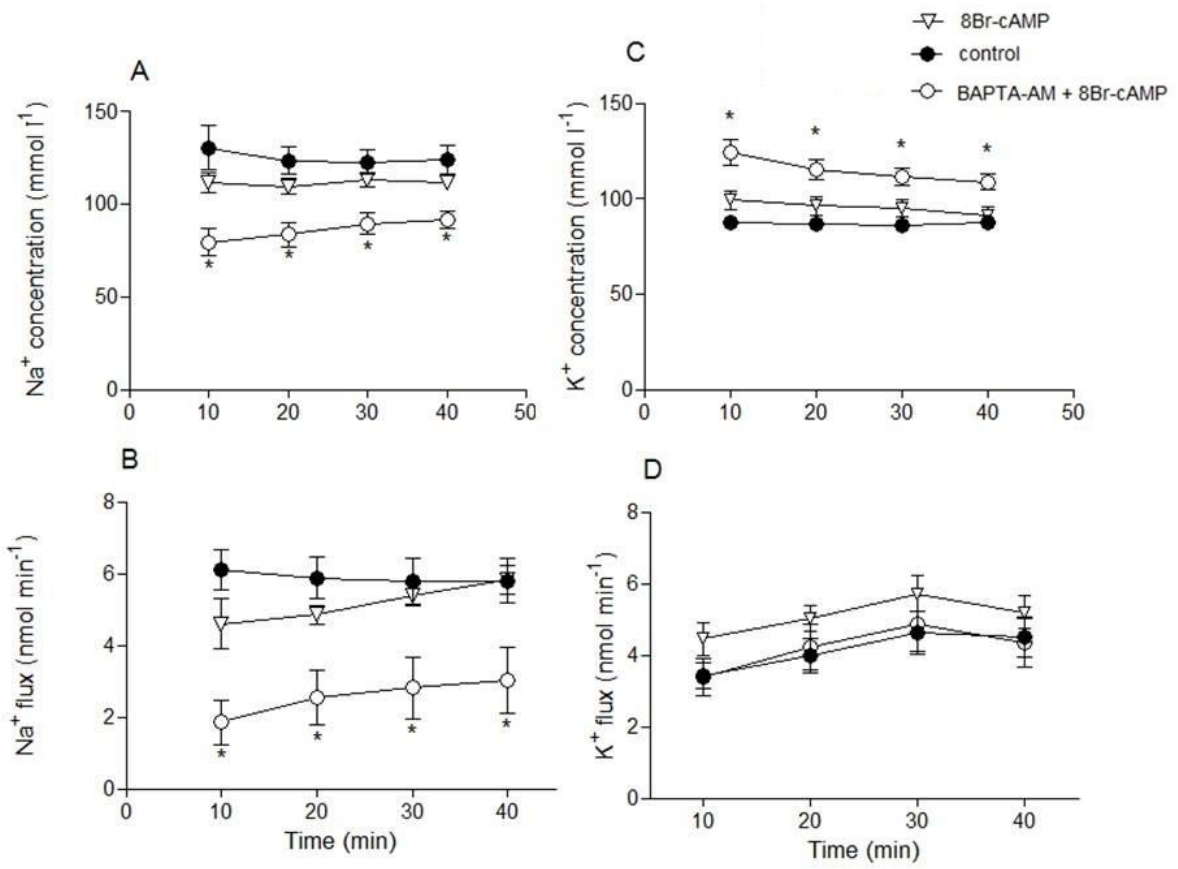

Figure 16: BAPTA-AM affects the ion composition of the secreted fluid from 8Br-cAMP stimulated tubules. Na^+ concentration (A) and flux (B) are significantly reduced in tubules incubated in Ca^{2+}-free saline plus 300 µmol l^{-1} BAPTA-AM (open circles) compared with both serotonin (filled circles) and 8Br-cAMP controls (open triangles, $p<0.05$, n=5 for 8Br-cAMP control group, n=7 for serotonin control group and n=11 for Ca^{2+}-free saline plus BAPTA-AM group, repeated measures two way ANOVA, Tukey-Kramer multiple comparison test). K^+ concentration (C) is increased and flux (D) is maintained in tubules incubated in Ca^{2+}-free saline plus 300 µmol l^{-1} BAPTA-AM compared with both serotonin and 8Br-cAMP controls ($p<0.05$, n=10 for cAMP control group, n=10 for serotonin control group and n=11 for $Ca2^+$-free saline plus BAPTA-AM group, repeated measures two way ANOVA, Tukey-Kramer multiple comparison test). Asterisks indicate significant difference. Bars represent SEM.

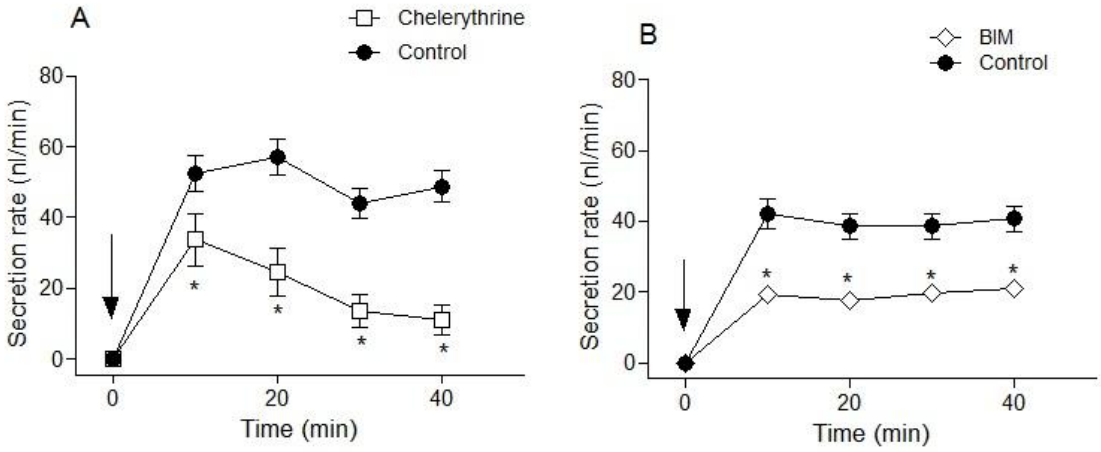

Figure 17: PKC blockers decreased serotonin stimulated secretion rate. MTs bathed in control saline, control saline plus 5 µmol l^{-1} chelerythrine (open square) and control saline plus 10 µmol l^{-1} BIM (open rhomboid), were stimulated with 1 µmol l^{-1} serotonin at time 0 (arrow). A: The PKC blocker chelerythrine decrease secretion rate in a time dependent manner ($p<0.001$, n=14 for serotonin control group, n=15 for 5 µmol l^{-1} chelerythrine treated group, repeated measures two way ANOVA, Tukey-Kramer multiple comparison test, asterisks indicate significant difference). B: Treatment with the PKC blocker BIM significantly decreased secretion rate about 40-50% ($p<0.001$, n=24 for serotonin control group, n=25 for 10 uM BIM treated group, repeated measures two way ANOVA, Tukey-Kramer multiple comparison test, asterisks indicate significant difference). Bars represent SEM.

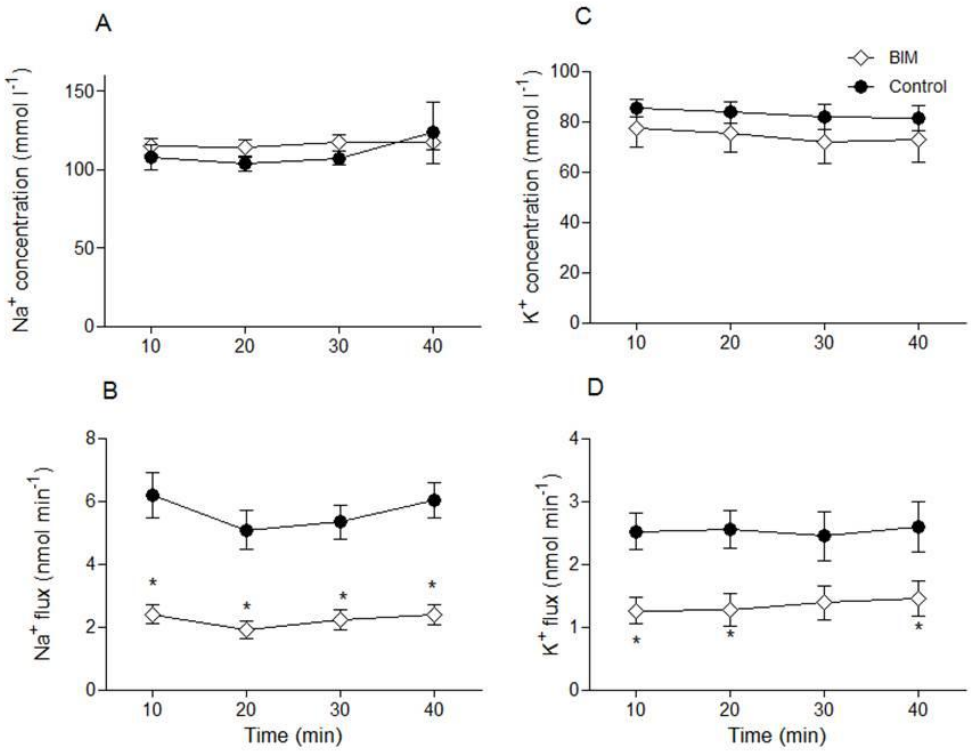

Figure 18: BIM affects Na^+ and K^+ concentration in the fluid secreted by serotonin stimulated tubules. Na^+ and K^+ were measured with ion selective electrodes. MTs bathed in control saline (filled circle) and control saline plus 10 µmol l^{-1} BIM (open rhomboid) were stimulated with 1 µmol l^{-1} serotonin. Na^+ concentration (A) remains the same while flux (B) is significantly reduced in tubules incubated in 10 µmol l^{-1} BIM ($p<0.001$, n=13 for controls, n=13 for BIM group, repeated measures two way ANOVA, Tukey-Kramer multiple comparison test). K^+ concentration (C) is unaffected while flux (D) is significantly decreased in tubules incubated with 10 µmol l^{-1} BIM ($p<0.05$, n=12 for controls, n=12 for BIM group, repeated measures two way ANOVA, Tukey-Kramer multiple comparison test). Asterisks indicate significant difference. Bars represent SEM.

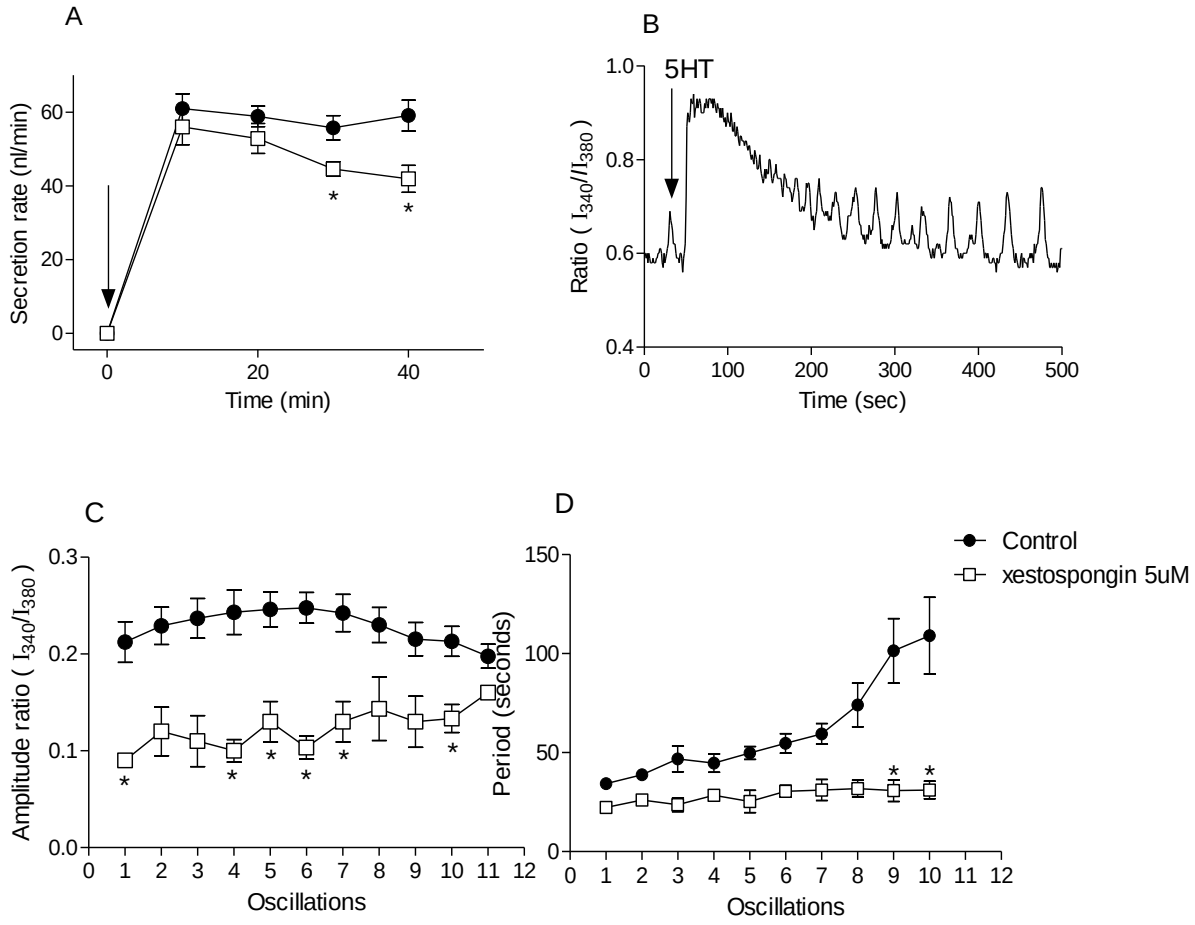

Figure 19: Xestospongin affects secretion rate and Ca^{2+} oscillations. MTs incubated in control saline (filled circle) or control saline plus 5 µmol l^{-1} xestospongin (open squares) were stimulated with 1 µmol l^{-1} serotonin at time 0 (arrow). A: Xestospongin slightly decreased fluid secretion rate. ($p<0.05$, n=6 for controls, n=8 for xestospongin). B: Ca^{2+} oscillation sample trace of a tubule treated with xestospongin after the addition of serotonin (arrow). C: Calcium waves amplitudes of xestospongin treated tubules showed significant differences with from those in serotonin stimulated tubules ($p<0.05$, n=13 for controls, n=4 for xestospongin). D: Frequency after stimulation. Xestospongin has a stable frequency in time while control group shows a decrease over time. (n=4 for xestospongin and n=13 for control). Repeated measures ANOVA, Tukey-Kramer multiple comparison test, asterisks indicate significant difference. Bars represent SEM.

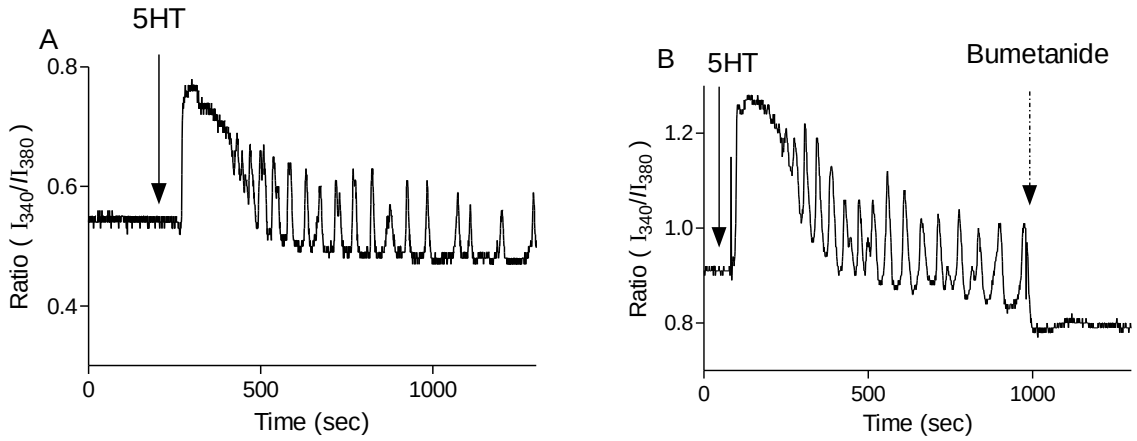

Figure 20: Bumetanide triggers a negative feedback loop from NKCC to Ca^{2+} stores. Tubules were incubated in Fura2-AM for 60 min and stimulated with 0.1 µmol l^{-1} serotonin (first arrow). A: Ca^{2+} oscillations after serotonin stimulation in tubules in control conditions. B: after serotonin stimulation 1 µmol l^{-1} bumetanide was added (first arrow). The addition of bumetanide consistently inhibited Ca^{2+} waves. This experiment was repeated 19 times with similar results.

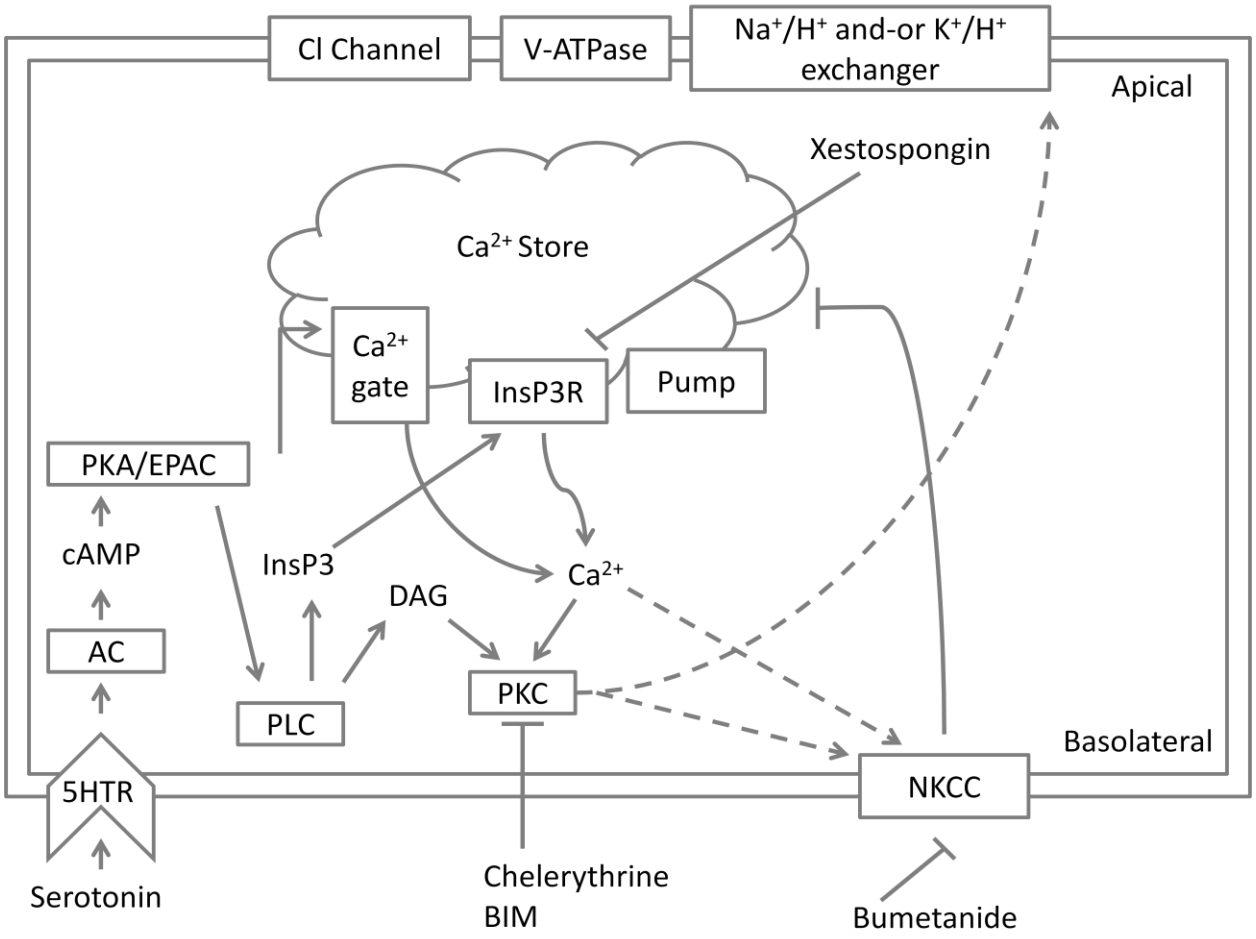

Figure 21: Proposed model. Serotonin binds to only one type of G protein coupled receptor that stimulates and AC. cAMP, product of AC stimulation, binds to the regulatory subunits of PKA activating it. Subsequently, PKA stimulates a phospholipase C (PLC) which increases Ins3P and DAG intracellular concentrations, triggering Ca^{2+} release and PKC activation respectively. The oscillatory nature of Ca^{2+} response requires pumps resulting in cytosolic Ca^{2+} decrease. PKA may also directly stimulate Ca^{2+} release. The study proposes a feedback mechanism from NKCC to the Ca^{2+} stores.

4. CONCLUSIONS AND DISCUSSION:

4.1. cAMP mediated Ca^{2+} waves

Taken together, the results indicate that serotonin stimulation of *R. prolixus* tubules involves both cAMP [17,22] and intracellular Ca^{2+} as second messengers. The importance of extracellular Ca^{2+} was tested by incubating the tubules in Ca^{2+}-free saline containing the Ca^{2+} chelator EGTA. EGTA-treated tubules didn't show significant differences in secretion rate as well as in the ion fluxes, suggesting extracellular Ca^{2+} doesn't play a role in the modulation of the ion transporters involved in diuresis in the distal segment of *R. prolixus* . Furthermore, tubules treated with EGTA showed Ca^{2+} oscillations in response to serotonin that had the same amplitude as those in control tubules. However, frequency of Malpighian tubules treated with EGTA was altered compared with controls. Overall, the results suggest that extracellular Ca^{2+} is not essential for a maximal secretory response.

It is known that Ca^{2+} waves frequency can optimize the activation of Ca^{2+} dependent proteins based on their Ca^{2+} binding constants [64]. Therefore, it was expected both in EGTA treated tubules and in cAMP stimulated tubules to find a modified secretory response. Why changes in Ca^{2+} frequency under these two treatments didn't change the secretory properties is not known. A possible hypothesis is that there is a minumun threshold for those changes; this could mean that Ca^{2+} activation mechanisms can support certain fluctuations. Another hypothesis is that frequency may be related with other cellular processes and not with the modulation of ion transporters in charge of primary urine production. I have no tested other physiological parameters more than the secretory process, therefore is possible that the change in Ca^{2+}

frequency is affecting another physiological function. Since cAMP and EGTA treatments show some consistencies in frequencies analysis a possible explanation is that the serotonin receptor not only activates an adenilate cyclase but somehow opens membrane Ca^{2+} channels, introducing extracellular Ca^{2+} into the cytoplasm. However, it is important to remember that this event doesn't seem to be related with the secretory process.

Treatment with membrane permeable Ca^{2+} chelator BAPTA-AM, was able to abrogate Ca^{2+} oscillations and reduce serotonin-stimulated secretion by 75%. These results suggest that Ca^{2+} from intracellular stores is necessary for maximal secretion in response to serotonin. This conclusion contradicts previous reports showing that treatment with the intracellular Ca^{2+} blocker TMB-8 does not affect serotonin-stimulated secretion in *R. prolixus* Malpighian tubules [28,45]. The reason for this inconsistency may be difficult to determine, however, it is possible that TMB-8 may not be an effective blocker of intracellular Ca^{2+} in this tissue. Alternatively, it is also possible that TMB-8 might be extruded from the cell by the Malpighian tubules. Thus, I conclude that serotonin stimulates, in addition to cAMP, intracellular Ca^{2+} second messenger pathways.

There are many types of serotonin receptor: most of them are G protein coupled receptors (GPCR) and work through cAMP. However, some of them work through Ca^{2+}. In the invertebrate *Caenorhabditis elegans*, serotonin receptor type 2 (5-HT_2), increases Ins3P, DAG and Ca^{2+} levels [65]. In *D. melanogaster* serotonin receptor type 7 (5-HT_7) elevates intracellular cAMP [65,66]. In *Calliphora vicina* salivary glands, 5-HT_2 stimulates Ca^{2+} signaling while and 5-HT_7 increases cAMP [38]. A possible explanation for my results is that serotonin binds to two different types of serotonin receptors, i.e. 5-HT_2 and 5-HT_7. However, 8Br-cAMP is able to trigger Ca^{2+} waves and ion transport identical to those obtained with serotonin, suggesting that

cAMP stimulates the same secretory response. Based on this information, it seems likely that cAMP acts upstream and not in parallel to Ca^{2+} release. Thus, it seems likely that serotonin activate only one type of serotonin receptor on *R. prolixus* Malpighian tubules, resulting in the activation of cAMP second messenger pathway that mediates Ca^{2+} release. This is the first demonstration of cAMP-dependent Ca^{2+} in Malpighian tubules. Is important to point out that further experiments are needed to support this hypothesis, for example the use of 5-carboxamidotryptamine, an 5HTR-$_7$ blocker, or 5-methoxytryptamine, a 5HTR-$_3$ blocker [38].

Malpighian tubules from other insects, including *D. melanogaster, L. migratoria* and *A. aegypti*, require activation of intracellular Ca^{2+} and cyclic nucleotide second messenger pathways to achieve maximal stimulation [28,51,67]. However, in these insects Ca^{2+} and cyclic nucleotide intracellular second messenger pathways are triggered by different diuretic hormones [28,51,67] . In the case of *R. prolixus*, both cAMP and Ca^{2+} are triggered by a single signal, i.e. serotonin. However, most of the research done in Malpighian tubules focuses on the ion transporter model more than in the regulatory mechanisms. How Ca^{2+} and nucleotides are able to modify the secretory processes of this epithelia is poorly understood.

The results in this study suggest that cAMP activates PLC, which subsequently hydrolyzes PIP2 into Ins3P and DAG. Isn3P triggers Ca^{2+} release while DAG activates PKC. The activation of PLC activation via cAMP pathway is not well understood and has only been described few times [68,69]. In this study, xestospongin treatment decreased the amplitude of the Ca^{2+} waves and PKC blockers diminished secretion rate. These results suggest that the PLC pathway is active in the serotonin-stimulated Malpighian tubules of *R. prolixus*. Interestingly, xestospongin did not abrogate Ca^{2+} oscillations, therefore, it is hypothesized that there is another

gate for Ca^{2+} besides InsP3Rs. The combined use of xestospongine and RyR antagonist could help to elucidate the identity of this Ca^{2+} gate.

These results support previous reports on Ca^{2+} modulation via cAMP. In mouse pancreatic β cells, Exchange Protein Activated by cAMP (Epac), and PKA directly activate or facilitate the opening InsP3Rs, RyRs and PLC [69]. In chromaffin cells, the activation of an adenylate cyclase (AC) causes intracellular Ca^{2+} release [70]. In human and mouse intestinal cells, Epac is described to activate a PLC with a subsequent Ca^{2+} release and PKC activation [58]. In mouse and human intestinal cells, Cl^- transport regulation are under cAMP and Ca^{2+}, but Ca^{2+} is downstream to cAMP [58] and in salivary glands of *C. vecina* serotonin increases cAMP, activating a PKA that could directly facilitate InsP3Rs Ca^{2+} release [39].

4.2. Role of PKC

PKC blockers chelerythrine and BIM decreased secretion rate. Analysis of the fluid secreted by BIM-treated tubules showed that Na^+ and K^+ concentration do not change compared to serotonin-stimulated tubules, suggesting all ions are being affected equally.

There are many types of PKC, the two main categories are conventional and novel PKCs. Conventional PKCs have two activation domains, one binds to Ca^{2+} and the other one binds to DAG. Novel PKCs do not need Ca^{2+} for activation [71]. The role of different PKCs in ion transport regulation is worth to mention since some of them seem to increase ion transport, and others seems to act in the opposite way. In T84 intestinal human cells, activation of PKCδ and PKCε, but not the conventional PKCα, decrease surface NKCC and therefore decrease Cl^- secretion [72,73]. However, a different study showed that PKCδ activate SPAK (Ste20-related proline alanine-rich kinase), which subsequently activates NKCC and therefore increases Cl^- transport [74].

similar pathways have been proposed in killifish opercular epithelia, where PKC is supposed to activate NKCC via SPAK/OSR1 [75]. In airway epithelia, NKCC activity has been reported to be PKCδ dependent through cytoskeleton modifications[76]. Bioinformatics analysis of mammalian NCC69 protein sequence, the *D. melanogaster* homolog of NKCC1, resulted in the same putative phosphorylation sites for PKA and PKC. Both PKA and PKC, in particular PKCδ, are reported to regulate the NKCC; however, no study has proven direct contact between these kinases and the cotransporter. The only kinases reported to directly interact with NKCC are SPAK/OSR1 [77–79].

Based on the results and the literature I hypothesized that Ca^{+} via PKA/Epac and PKC regulates the NKCC and, possibly, the Na^{+}/H^{+} exchanger. *In vitro* experiments in mammalian renal vesicles reported that PKA directly downregulates Na^{+}/H^{+} exchanger while PKC directly activates the exchanger [80]. In the intestinal cell line C2BBe1, PKCδ increases the activity of a Na^{+}/H^{+} exchanger [81]. In this study, it was demonstrated that PKC is essential to obtain maximal secretion rate in Malpighian tubules from *R. prolixus*, however, the identity of that PKC and the specific role are not completely addressed. I propose the working hypothesis that PKC regulates the NKCC, the Na^{+}/H^{+} exchanger or both.

4.3. Ca^{2+} and NKCC

The results in this study suggest that Ca^{2+} plays a role in modulating the activity of at least one of ion transport processes involved in ion and fluid secretion. The effect of serotonin on the Cl^{-} channel, V-type H^{+}-ATPase and NKCC cotransporter was tested using TEP measurements. The experiments suggest that the lack Ca^{2+} affects the activation of basolateral NKCC cotransporter. This hypothesis is further supported by measurements of secreted fluid ion

composition. The results showed that incubation in Ca^{2+}-free saline plus BAPTA-AM increased K^+ concentration in the secreted fluid while Na^+ concentration decreased. This result is similar to that obtained by treatment with the NKCC cotransporter blockers bumetanide or furosemide [12,22]. Inhibition of the NKCC cotransporter with furosemide results in an increase in the concentration of K^+ and a decrease of Na^+ concentration in the secreted fluid [20,22]. Thus, the data supports the hypothesis that tubules incubated with Ca^{2+}-free saline containing BAPTA-AM have a reduced NKCC activity. The mechanism of Ca^{2+} regulation of NKCC activity is not understood. However, as mentioned before, NKCC activity has been correlated with PKC activation in several tissue [74,76]. NKCC1 has putative phosphorylation sites for PKC; in fact PKC activity has been associated with NKCC activation [61,82].Direct phosphorylation of PKC on the NKCC has never been proved but indirectly, PKCδ, is known to activate SPAK, leading to NKCC upregulation [74]. It is important to point out that BAPTA-AM treated tubules showed similar but not identical results to tubules treated with the PKC blocker BIM, suggesting additional roles for Ca^{2+} in the secretory response. Na^+ and K^+ transport into the lumen is mediated by an amiloride-sensitive Na^+/H+ and K^+/H^+ exchanger(s) [22]. Incubation with Ca^{2+}-free saline plus BAPTA-AM causes drop in the secreted fluid pH, suggesting that the apical Na^+ and K^+/H^+ exchanger(s) activity is also reduced. Similarly, treatment with amiloride causes the pH of the secreted fluid to decrease by a unit [22]. As mentioned before, in mammalian intestine cells [80], bacteria [83] and goldfish somatotropes [84]PKC activates Na^+ and K^+/H^+ exchangers. However, this drop in pH can be also explained through the reduction in the NKCC activity[34,85,86]. If Na^+ doesn't enter the cell from the basolateral membrane, the apical Na^+/H^+ exchanger must stop working, leading H^+ accumulation in the lumen, product of the V-ATPase activity, and acidic pH,.

4.4. The ion sensor

It is unlikely that a system as complex as the one in Malpighian tubules of *R. prolixus* present a simple "ON-OFF" regulation. *R. prolixus* can feed on different animals' blood, changing their hemolymph composition in each blood meal. The ion transport machinery has evolved to deal with different salt loads. The Malpighian tubules respond to sudden changes in Na^+ and K^+ loads in the hemolymph by changing the amount of Na^+ or K^+ been excreted [48]. For example, a 80% reduction in K^+ content in the fluid bathing the tubules causes a 20% reduction in K^+ transport rate and a barely noticeable 2% change in intracellular K^+ [48]. These changes take place in less than 3 seconds. These large changes in transepithelial ion flux in response to sudden changes in the Na^+ or K^+ content in the hemolymph, while maintaining intracellular ion constant, likely requires intracellular regulatory machinery. In other systems there is evidence of the existence of intracellular "ion sensors" that directs the fine regulation of ion transporters/channels after the initial onset [32,87].

The results showed that Ca^{2+} waves are modified after the treatment with the NKCC blocker bumetanide to serotonin-stimulated tubules. Bumetanide treatment changes intracellular ion composition by blocking the entrance of Na^+, K^+ and Cl. These results suggest that in *R. prolixus* Malpighian tubules there may be an ion sensing system that regulates the Ca^{2+} waves. It is possible that Ca^{2+} waves are involved in the coordination between channels and transporters that take part in transepithelial ion transport. A working hypothesis is that serotonin stimulation triggers intracellular Ca^{2+} waves and those waves are regulated by feedback mechanisms that sense intracellular ion composition. For that hypothesis is essential the existence of an ion sensor. Based on the literature this ion sensor could be regulating the fine tuning of the ion transporters activity after fluid secretion has been initiated[85]. The identity or mechanisms of this

hypothetical ion sensor is still unknown, however, there are some suspected pathways worthy to be explored. An ideal candidate for the "ion sensor" role is the With-No-Lysine-Kinase (WNK) pathway, which main role is to regulate chloride transporters (e.g. NKCC) and recently has been correlated with a Ca^{2+} binding protein [34,86]. WNKs were discovered in 2000 by Cobb and colleagues in the search for new members of the mitogen activated protein kinases, but they comprise a unique branch in the kinome [88,89]. The best described function of WNK1 is the regulation intracellular chloride and cell tonicity. For that purpose; WNK1 phosphorylates two Ste20p like Kinases, SPAK and Oxidative stress-responsive kinase (OSR) 1, which subsequently phosphorylate different ion channels such NKCC and K^+:Cl^- cotransporters (KCC) [77,85].

4.5. Proposed model (Figure 21):

Based on the results, it seems that both cAMP and PLC-PKC pathway are involved in serotonin stimulated secretion. However cAMP stimulation is enough for maximal secretion rate. Therefore PLC-PKC must act downstream cAMP. Based on those results we hypothesize that serotonin binds a GPCR, increasing cAMP by activation of an adenylate cyclase (AC). Subsequently, cAMP binds to PKA or Epac regulatory subunits releasing the catalytic ones. cAMP is somehow able to activate PLC, which finally produces Ca^{2+} release, PKC activation and NKCC upregulation. Na^+/H^+ exchanger could also be upregulated by PKC. Since xestospongin treatment didn't abrogate Ca^{2+} waves, an alternative pathway for Ca^{2+} release must also be operating. Direct regulation of cAMP on intracellular Ca^{2+} stores by RyRs regulation has been reported [90].

4.6. Calcium waves:

Ca^{2+} is an important second messenger in the signal transduction of many cell types of different species. Cytoplasmic Ca^{2+} concentration above 100 nmol l^{-1} is incompatible with life [91]. Therefore, early in evolution, cells developed a system to limit cytoplasmic Ca^{2+}. This system created a concentration gradient that was later evolved as one of the most widespread signaling processes.

Ca^{2+} is a signaling transduction process of many polarized secretory epithelial cells, triggered by hormonal or neurotransmitter stimulation, that regulate different ion transporters such as NKCC and Na^{+}/H^{+} exchanger [34,80,83,86,92].

Ca^{2+} reservoirs for signaling in cells are: the extracellular space, mitochondria and endoplasmic reticulum (ER). However, the most described and robust source of Ca^{2+} described in secretory epithelia seems to be the ER [93–95]. In the ER, there are two types of Ca^{2+} channels described to participate in Ca^{2+} release: InsP3R and ryanodine receptors (RyR).

Even though the role is less clear, the mitochondria have been reported to be involved in calcium signaling. In frog early distal tube [94,95] and adrenal chromaffin cells [96] , among others. Mitochondria modulates the spatially and temporal properties of Ca^{2+} signals. This regulation seems to rely in the Ca^{2+} reuptake properties of the mitochondria after release from the ER [32,94,95,97]. It is noteworthy that mitochondria and ER are physically connected in many cell types. Mitochondria-associated ER membranes (MAMs) shows micro-domains from where the mitochondria is able to, uptake Ca^{2+} directly from InsP3Rs [97]. In *R. prolixus* Malpighian tubules Ca^{2+} waves are InsP3Rs dependent, but it is hypothesized that there is at least one other Ca^{2+} source.

Usually, Ca^{2+} oscillations start in the apical region of the cells and propagate to the basolateral side [93]. A particular characteristic of Ca^{2+} oscillations is the presence of "pioneer cells". These cells seem to initiate the response and coordinate the signal to the neighboring cells [98]. This evidence suggests there are cells that could be more sensitive than other to the initiation of the response. There are at least two different reasons why these pioneer cells can be more responsive; a higher density of agonist receptor in the membrane or a higher abundance of intracellular Ca^{2+} release channels [99].The Ca^{2+} oscillations displayed by *R. prolixus* Malpighian tubules after serotonin stimulation showed that some cells are more reactive than others, i.e. pioneer cells[93,100], and that those cells seem to propagate the signal to neighbors cells. Pioneer cells have been found in many tissues from *R. prolixus* to mammalian cells [93]. However, the functionality of pioneer cells and how the Ca^{2+} signal is propagated needs further research. It was noticed in our analysis that the propagation occurs from distal to proximal. Therefore, an hypothesis worth to investigate is that may be the propagation of Ca^{2+} waves correlates with a sequential activation of the ion transporter machinery on each cell. Under this hypothesis there would be secretory flux oscillations. This set up could work to impulse the primary urine flow to the proximal sector of the tubule. This hypothesis could be tested using the Scanning Ion-selective Electrode Technique (SIET).

The amplitude and/or frequency of Ca^{2+} waves may encode physiological relevant information. In some tissues is the change in amplitude that modulates physiological responses while in other it is the frequency. In this study I analyzed both parameters of the Ca^{2+} oscillations in response to serotonin in Malpighian tubules of *R prolixus*. EGTA and 8-Br-cAMP treatments produce differences in Ca^{2+} waves frequency of *R. prolixus* when compare to control tubules. However, under the conditions and timeline studied, these changes do not seem to have

physiological consequences in the secretory response since secretion rate and ion transport were unaffected under these treatments. Xestospongin produced changes in both parameters, changing also the physiological response (i.e. decreased secretion rate). These results suggest that it is the amplitude, rather than the frequency of the Ca^{2+} waves that correlate with physiological changes, thus suggesting that amplitude is the physiological relevant parameter in *R. prolixus*.

Ca^{2+} waves generated in this study are, in general, prior to the observation of droplets in the secretion assay. However, it must be noticed that the secretion process starts before droplet collection. For a droplet to be collected, the secretion has to, first, overcome the oil surface tension. Second, has to be big enough to be safely collected. Under these circumstances is not possible to address the question of whether the generation of Ca^{2+} waves occurs before or concomitant to secretion. It can be said, however, that Ca^{+} waves are essential and may be one of the first events in the signaling cascade of diuresis in Malpighian tubules of *R prolixus*.

This is the very first time that diuresis in *R prolixus* is reported to be Ca^{2+} dependant. These results are critical to the understanding of one of the major postprandial events in this insect. A deeper knowledge in the regulatory processes of can lead to the development of new pesticides, reducing Chagas' disease transmission. Here I present a first insight into the role of Ca^{2+} in the diuretic process of this insect, hoping it will encourage researchers to continue with work.

5. REFERENCES:

1. *Insect physiology and biochemistry*. **1**, 485 (CRC PressINC: 2002).

2. *The Insects: Structure and Function*. **2012**, 954 (Cambridge University Press: 2012).

3. Nijhout, H. F. *Insect Hormones*. 267 (Princeton University Press: 1998).

4. Klowden, M. J. *Physiological Systems in Insects*. 688 (Academic Press: 2010).

5. *Encyclopedia of Entomology, Volume 4*. 4346 (Springer: 2008).

6. *The Biology of Disease Vectors*. 785 (Elsevier Academic Press: 2005).

7. Sargsyan, V. *et al.* Phosphorylation via PKC Regulates the Function of the Drosophila Odorant Co-Receptor. *Frontiers in cellular neuroscience* **5**, 5 (2011).

8. Suarez, R. K. Oxygen and the upper limits to animal design and performance. *The Journal of experimental biology* **201**, 1065–72 (1998).

9. Suarez, R. K. Upper limits to mass-specific metabolic rates. *Annual review of physiology* **58**, 583–605 (1996).

10. Makarieva, A. M. *et al.* Mean mass-specific metabolic rates are strikingly similar across life's major domains: Evidence for life's metabolic optimum. *Proceedings of the National Academy of Sciences of the United States of America* **105**, 16994–9 (2008).

11. *Encyclopedia of Insects*. 1024 (Academic Press: 2009)

12. Ianowski, J. P., Christensen, R. J. & O'Donnell, M. J. Intracellular ion activities in Malpighian tubule cells of Rhodnius prolixus: evaluation of Na+-K+-2Cl- cotransport across the basolateral membrane. *The Journal of experimental biology* **205**, 1645–1655 (2002).

13. Wigglesworth, V. B. & Salpeter, M. M. Histology of the Malpighian tubules in Rhodnius prolixus Stål (Hemiptera). *Journal of Insect Physiology* **8**, 299–307 (1962).

14. Buxton, P. A. The biology of a blood-sucking bug, Rhodnius prolixus. *Transactions of the Royal Entomological Society of London* **78**, 227–256 (1930).

15. Ianowski, J. P., Manrique, G., Núñez, J. A. & Lazzari, C. R. Feeding is not necessary for triggering plasticization of the abdominal cuticle in haematophagous bugs. *Journal of insect physiology* **44**, 379–384 (1998).

16. Coast, G. M. *et al.* Neurohormones implicated in the control of Malpighian tubule secretion in plant sucking heteropterans: The stink bugs Acrosternum hilare and Nezara viridula. *Peptides* **31**, 468–73 (2010).

17. Te Brugge, V. A., Schooley, D. A., Orchard, I. & Brugge, V. A. Te The biological activity of diuretic factors in Rhodnius prolixus. *Peptides* **23**, 671–681 (2002).

18. Maddrell, S. H., Herman, W. S., Mooney, R. L. & Overton, J. A. 5-Hydroxytryptamine: a second diuretic hormone in Rhodnius prolixus. *The Journal of experimental biology* **156**, 557–566 (1991).

19. O'Donnell, M. J. & Maddrell, S. H. Paracellular and transcellular routes for water and solute movements across insect epithelia. *The Journal of experimental biology* **106**, 231–53 (1983).

20. Ianowski, J. P. & O'Donnell, M. J. Transepithelial potential in Malpighian tubules of Rhodnius prolixus: lumen-negative voltages and the triphasic response to serotonin. *Journal of insect physiology* **47**, 411–421 (2001).

21. Ianowski, J. P. & O'Donnell, M. J. Electrochemical gradients for Na+, K+, Cl- and H+ across the apical membrane in Malpighian (renal) tubule cells of Rhodnius prolixus. *The Journal of experimental biology* **209**, 1964–1975 (2006).

22. Maddrell, S. H. & O'Donnell, M. J. Insect malpighian tubules: v-atpase action in ion and fluid transport. *The Journal of experimental biology* **172**, 417–429 (1992).

23. Staniscuaski, F., Paluzzi, J.-P., Real-Guerra, R., Carlini, C. R. & Orchard, I. Expression analysis and molecular characterization of aquaporins in Rhodnius prolixus. *Journal of insect physiology* (2013).doi:10.1016/j.jinsphys.2013.08.013

24. Maddrell, S. H. Excretion in the Blood-Sucking Bug, Rhodnius Prolixus Stal. Ii. the Normal Course of Diuresis and the Effect of Temperature. *The Journal of experimental biology* **41**, 163–176 (1964).

25. Maddrell, S. H. Excretion in the blood-sucking bug, Rhodnius prolixus stal. 3. The control of the release of the diuretic hormone. *The Journal of experimental biology* **41**, 459–72 (1964).

26. Maddrell, S. H. P. The fastest fluid-secreting cell known: The upper malpighian tubule of Rhodnius. *BioEssays* **13**, 357–362 (1991).

27. O'Donnell, M. J., Ianowski, J. P., Linton, S. M. & Rheault, M. R. Inorganic and organic anion transport by insect renal epithelia. *Biochimica et biophysica acta* **1618**, 194–206 (2003).

28. Paluzzi, J. P. *et al.* Investigation of the potential involvement of eicosanoid metabolites in anti-diuretic hormone signaling in Rhodnius prolixus. *Peptides* **34**, 127–134 (2012).

29. *American Trypanosomiasis: Chagas Disease One Hundred Years of Research*

30. Levine, R. R. *Case Studies in Global Health: Millions Saved*. 172 (Jones & Bartlett Publishers: 2007)

31. *Chagas Disease, Part 1* . 390 (Academic Press: 2011). 32. Cooper, G. J., Fowler, M. & Hunter, M. Membrane cross-talk in the early distal tubule segment of frog kidney: role of calcium stores and chloride. *Pflugers Archiv : European journal of physiology* **442**, 243–247 (2001).

33. Reynolds, A. *et al.* Dynamic and differential regulation of NKCC1 by calcium and cAMP in the native human colonic epithelium. *The Journal of physiology* **582**, 507–524 (2007).

34. Shin, J.-H., Namkung, W., Choi, J. Y., Yoon, J.-H. & Lee, M. G. Purinergic stimulation induces Ca2+-dependent activation of Na+-K+-2Cl- cotransporter in human nasal epithelia. *The Journal of biological chemistry* **279**, 18567–74 (2004).

35. Capasso, G. *et al.* The calcium sensing receptor modulates fluid reabsorption and acid secretion in the proximal tubule. *Kidney international* **84**, 277–84 (2013).

36. Pollock, V. P. *et al.* NorpA and itpr mutants reveal roles for phospholipase C and inositol (1,4,5)- trisphosphate receptor in Drosophila melanogaster renal function. *The Journal of experimental biology* **206**, 901–911 (2003).

37. Yu, M. J. & Beyenbach, K. W. Leucokinin activates Ca(2+)-dependent signal pathway in principal cells of Aedes aegypti Malpighian tubules. *American journal of physiology.Renal physiology* **283**, F499–508 (2002).

38. Röser, C. *et al.* Molecular and pharmacological characterization of serotonin 5-HT2alpha and 5-HT7 receptors in the salivary glands of the blowfly Calliphora vicina. *PloS one* **7**, e49459 (2012).

39. Fechner, L., Baumann, O. & Walz, B. Activation of the cyclic AMP pathway promotes serotonin-induced Ca2+ oscillations in salivary glands of the blowfly Calliphora vicina. *Cell calcium* **53**, 94–101 (2013).

40. Coast, G. Serotonin has kinin-like activity in stimulating secretion by Malpighian tubules of the house cricket Acheta domesticus. *Peptides* **32**, 500–508 (2011).

41. Beyenbach, K. W. Transport mechanisms of diuresis in Malpighian tubules of insects. *The Journal of experimental biology* **206**, 3845–3856 (2003).

42. Radford, J. C., Terhzaz, S., Cabrero, P., Davies, S.-A. & Dow, J. A. T. Functional characterisation of the Anopheles leucokinins and their cognate G-protein coupled receptor. *The Journal of experimental biology* **207**, 4573–86 (2004).

43. Terhzaz, S. *et al.* Mechanism and function of Drosophila capa GPCR: a desiccation stress-responsive receptor with functional homology to human neuromedinU receptor. *PloS one* **7**, e29897 (2012).

44. Paluzzi, J. P., Naikkhwah, W. & O'Donnell, M. J. Natriuresis and diuretic hormone synergism in R. prolixus upper Malpighian tubules is inhibited by the anti-diuretic hormone, RhoprCAPA-alpha2. *Journal of insect physiology* **58**, 534–542 (2012).

45. Ruiz-Sanchez, E., Orchard, I. & Lange, A. B. Effects of the cyclopeptide mycotoxin destruxin A on the Malpighian tubules of Rhodnius prolixus (Stal). *Toxicon : official journal of the International Society on Toxinology* **55**, 1162–1170 (2010).

46. O'Donnell, M. J., Fletcher, M. & Haley, C. A. KCl reabsorption by the lower malpighian tubule of rhodnius prolixus: inhibition by Cl(-) channel blockers and acetazolamide. *Journal of insect physiology* **43**, 657–665 (1997).

47. Donini, A., O'Donnell, M. J. & Orchard, I. Differential actions of diuretic factors on the Malpighian tubules of Rhodnius prolixus. *The Journal of experimental biology* **211**, 42–8 (2008).

48. Ianowski, J. P., Christensen, R. J. & O'Donnell, M. J. Na+ competes with K+ in bumetanide-sensitive transport by Malpighian tubules of Rhodnius prolixus. *The Journal of experimental biology* **207**, 3707–16 (2004).

49. O'Donnell, M. J. & Maddrell, S. H. Fluid reabsorption and ion transport by the lower Malpighian tubules of adult female Drosophila. *The Journal of experimental biology* **198**, 1647–1653 (1995).

50. Dantzler, W. H. & Bentley, S. K. High K+ effects on PAH transport and permeabilities in isolated snake renal tubules. *The American journal of physiology* **229**, 191–9 (1975).

51. O'Donnell, M. J., Dow, J. A., Huesmann, G. R., Tublitz, N. J. & Maddrell, S. H. Separate control of anion and cation transport in malpighian tubules of Drosophila Melanogaster. *The Journal of experimental biology* **199**, 1163–1175 (1996).

52. Vázquez-Martínez, O., Cañedo-Merino, R., Díaz-Muñoz, M. & Riesgo-Escovar, J. R. Biochemical characterization, distribution and phylogenetic analysis of Drosophila melanogaster ryanodine and IP3 receptors, and thapsigargin-sensitive Ca2+ ATPase. *Journal of cell science* **116**, 2483–94 (2003).

53. Linton, S. M. & O'Donnell, M. J. Novel aspects of the transport of organic anions by the malpighian tubules of Drosophila melanogaster. *The Journal of experimental biology* **203**, 3575–3584 (2000).

54. Miyauchi, J. T., Piermarini, P. M., Yang, J. D., Gilligan, D. M. & Beyenbach, K. W. Roles of PKC and phospho-adducin in transepithelial fluid secretion by Malpighian tubules of the yellow fever mosquito. *Tissue Barriers* **1**, 20–19 (2013).

55. Coast, G. M. Neuroendocrine control of ionic homeostasis in blood-sucking insects. *The Journal of experimental biology* **212**, 378–86 (2009).

56. Montoreano, R., Triana, F., Abate, T. & Rangel-Aldao, R. Cyclic AMP in the Malpighian tubule fluid and in the urine of Rhodnius prolixus. *General and comparative endocrinology* **77**, 136–142 (1990).

57. Yao, L. *et al.* Dopamine and ethanol cause translocation of epsilonPKC associated with epsilonRACK: cross-talk between cAMP-dependent protein kinase A and protein kinase C signaling pathways. *Molecular pharmacology* **73**, 1105–12 (2008).

58. Hoque, K. M. *et al.* Epac1 mediates protein kinase A-independent mechanism of forskolin-activated intestinal chloride secretion. *The Journal of general physiology* **135**, 43–58 (2010).

59. Grandoch, M., Roscioni, S. S. & Schmidt, M. The role of Epac proteins, novel cAMP mediators, in the regulation of immune, lung and neuronal function. *British journal of pharmacology* **159**, 265–84 (2010).

60. Beraldo, F. H., Almeida, F. M., Da Silva, A. M. & Garcia, C. R. S. Cyclic AMP and calcium interplay as second messengers in melatonin-dependent regulation of Plasmodium falciparum cell cycle. *The Journal of cell biology* **170**, 551–7 (2005).

61. Marshall, W. S., Ossum, C. G. & Hoffmann, E. K. Hypotonic shock mediation by p38 MAPK, JNK, PKC, FAK, OSR1 and SPAK in osmosensing chloride secreting cells of killifish opercular epithelium. *The Journal of experimental biology* **208**, 1063–1077 (2005).

62. Larsen, A. K., Jensen, B. S. & Hoffmann, E. K. Activation of protein kinase C during cell volume regulation in Ehrlich mouse ascites tumor cells. *Biochimica et biophysica acta* **1222**, 477–482 (1994).

63. Geng, Y., Hoke, A. & Delpire, E. The Ste20 Kinases Ste20-related Proline-Alanine-rich Kinase and Oxidative-stress Response 1 Regulate NKCC1 Function in Sensory Neurons *. **284**, 14020–14028 (2009).

64. Marhl, M., Perc, M. & Schuster, S. A minimal model for decoding of time-limited Ca2+ oscillations. *Biophysical chemistry* **120**, 161–7 (2006).

65. Tierney, A. J. Structure and function of invertebrate 5-HT receptors: a review. *Comparative biochemistry and physiology. Part A, Molecular & integrative physiology* **128**, 791–804 (2001).

66. Saudou, F., Boschert, U., Amlaiky, N., Plassat, J. L. & Hen, R. A family of Drosophila serotonin receptors with distinct intracellular signalling properties and expression patterns. *The EMBO journal* **11**, 7–17 (1992).

67. Morgan, P. J. & Mordue, W. 5-Hydroxytryptamine stimulates fluid secretion in locust malpighian tubules independently of cAMP. *Comparative biochemistry and physiology.C, Comparative pharmacology and toxicology* **79**, 305–310 (1984).

68. Gomes, P. & Soares-da-Silva, P. Role of cAMP-PKA-PLC signaling cascade on dopamine-induced PKC-mediated inhibition of renal Na(+)-K(+)-ATPase activity. *American journal of physiology. Renal physiology* **282**, F1084–96 (2002).

69. Dzhura, I. *et al.* Phospholipase C-ε links Epac2 activation to the potentiation of glucose-stimulated insulin secretion from mouse islets of Langerhans. *Islets* **3**, 121–8 (2011).

70. Hamelink, C., Lee, H.-W., Chen, Y., Grimaldi, M. & Eiden, L. E. Coincident elevation of cAMP and calcium influx by PACAP-27 synergistically regulates vasoactive intestinal polypeptide gene transcription through a novel PKA-independent signaling pathway. *The Journal of neuroscience : the official journal of the Society for Neuroscience* **22**, 5310–20 (2002).

71. Farah, C. A. & Sossin, W. S. The Role of C2 Domains in PKC Signaling; Calcium Signaling. **740**, 663–683 (2012).

72. Song, J. C., Hrnjez, B. J., Farokhzad, O. C. & Matthews, J. B. PKC-epsilon regulates basolateral endocytosis in human T84 intestinal epithelia: role of F-actin and MARCKS. *Am J Physiol Cell Physiol* **277**, C1239–1249 (1999).

73. Tang, J. *et al.* Activated PKC{delta} and PKC{epsilon} inhibit epithelial chloride secretion response to cAMP via inducing internalization of the Na+-K+-2Cl- cotransporter NKCC1. *The Journal of biological chemistry* **285**, 34072–34085 (2010).

74. Smith, L., Smallwood, N., Altman, A. & Liedtke, C. M. PKCdelta acts upstream of SPAK in the activation of NKCC1 by hyperosmotic stress in human airway epithelial cells. *The Journal of biological chemistry* **283**, 22147–22156 (2008).

75. Grosell, M., Larsen, E. H., Hoffmann, E. K. K., Schettino, T. & Marshall, W. S. S. The role of volume-sensitive ion transport systems in regulation of epithelial transport. *Includes papers presented in the session "Water Transport" at the Society of Experimental Biology's Annual Meeting at the University of Kent, Canterbury, UK, April 2nd–7th 2006* **148**, 29–43 (2007).

76. Liedtke, C. M., Hubbard, M. & Wang, X. Stability of actin cytoskeleton and PKC-delta binding to actin regulate NKCC1 function in airway epithelial cells. *American journal of physiology. Cell physiology* **284**, C487–96 (2003).

77. Gagnon, K. B., England, R. & Delpire, E. Characterization of SPAK and OSR1, regulatory kinases of the Na-K-2Cl cotransporter. *Molecular and cellular biology* **26**, 689–698 (2006).

78. Thastrup, J. O. *et al.* SPAK/OSR1 regulate NKCC1 and WNK activity: analysis of WNK isoform interactions and activation by T-loop trans-autophosphorylation. *The Biochemical journal* **441**, 325–37 (2012).

79. Gagnon, K. B. & Delpire, E. Molecular physiology of SPAK and OSR1: two Ste20-related protein kinases regulating ion transport. *Physiological reviews* **92**, 1577–617 (2012).

80. Weinman, E. J., Dubinsky, W. & Shenolikar, S. Regulation of the renal Na+-H+ exchanger by protein phosphorylation. *Kidney international* **36**, 519–25 (1989).

81. Muthusamy, S. *et al.* PKCδ-dependent activation of ERK1/2 leads to upregulation of the human NHE2 transcriptional activity in intestinal epithelial cell line C2BBe1. *American journal of physiology. Gastrointestinal and liver physiology* **302**, G317–25 (2012).

82. Del Castillo, I. C. *et al.* Dynamic regulation of Na(+)-K(+)-2Cl(-) cotransporter surface expression by PKC-{epsilon} in Cl(-)--secretory epithelia. *American journal of physiology.Cell physiology* **289**, C1332–42 (2005).

83. Hodges, K., Gill, R., Ramaswamy, K., Dudeja, P. K. & Hecht, G. Rapid activation of Na+/H+ exchange by EPEC is PKC mediated. *American journal of physiology. Gastrointestinal and liver physiology* **291**, G959–68 (2006).

84. Li, G.-L., Parks, S. K., Goss, G. G. & Chang, J. P. PKC mediates GnRH activation of a Na+/H+ exchanger in goldfish somatotropes. *General and comparative endocrinology* **166**, 296–306 (2010).

85. Mccormick, J. A. & Ellison, D. H. The WNKs : Atypical Protein Kinases With Pleiotropic Actions. **91**, 177–219 (2011).

86. Ponce-Coria, J., Gagnon, K. B. & Delpire, E. Calcium-binding protein 39 facilitates molecular interaction between Ste20p proline alanine-rich kinase and oxidative stress response 1 monomers. *American journal of physiology. Cell physiology* **303**, C1198–205 (2012).

87. Kahle, K. T., Rinehart, J. & Lifton, R. P. Phosphoregulation of the Na-K-2Cl and K-Cl cotransporters by the WNK kinases. *Biochimica et biophysica acta* **1802**, 1150–8 (2010).

88. Huang, C.-L., Yang, S.-S. & Lin, S.-H. Mechanism of regulation of renal ion transport by WNK kinases. *Current opinion in nephrology and hypertension* **17**, 519–25 (2008).

89. Kahle, K. T., Ring, A. M. & Lifton, R. P. Molecular physiology of the WNK kinases. *Annual review of physiology* **70**, 329–55 (2008).

90. Reiken, S. *et al.* PKA phosphorylation activates the calcium release channel (ryanodine receptor) in skeletal muscle: defective regulation in heart failure. *The Journal of cell biology* **160**, 919–28 (2003).

91. Case, R. M. *et al.* Evolution of calcium homeostasis: from birth of the first cell to an omnipresent signalling system. *Cell calcium* **42**, 345–50 (2007).

92. Fowler, M. R., Cooper, G. J. & Hunter, M. Regulation and identity of intracellular calcium stores involved in membrane cross talk in the early distal tubule of the frog kidney. *American journal of physiology.Renal physiology* **286**, F1219–25 (2004).

93. Ashby, M. C. & Tepikin, A. V Polarized calcium and calmodulin signaling in secretory epithelia. *Physiological reviews* **82**, 701–34 (2002).

94. Fowler, M. R. & Hunter, M. Mitochondrial Ca2+ transport in frog early distal tubule. *Experimental physiology* **90**, 195–201 (2005).

95. Fowler, M. R., Cooper, G. J. & Hunter, M. Regulation and identity of intracellular calcium stores involved in membrane cross talk in the early distal tubule of the frog kidney. *American journal of physiology.Renal physiology* **286**, F1219–25 (2004).

96. Herrington, J., Park, Y. B., Babcock, D. F. & Hille, B. Dominant role of mitochondria in clearance of large Ca2+ loads from rat adrenal chromaffin cells. *Neuron* **16**, 219–28 (1996).

97. Patergnani, S. *et al.* Calcium signaling around Mitochondria Associated Membranes (MAMs). *Cell communication and signaling : CCS* **9**, 19 (2011).

98. Segawa, A., Takemura, H. & Yamashina, S. Calcium signalling in tissue: diversity and domain-specific integration of individual cell response in salivary glands. *Journal of cell science* **115**, 1869–76 (2002).

99. Vorum, H., Hager, H., Christensen, B. M., Nielsen, S. & Honoré, B. Human calumenin localizes to the secretory pathway and is secreted to the medium. *Experimental cell research* **248**, 473–81 (1999).

100. Yamamoto-Hino, M. *et al.* Apical vesicles bearing inositol 1,4,5-trisphosphate receptors in the Ca2+ initiation site of ductal epithelium of submandibular gland. *The Journal of cell biology* **141**, 135–42 (1998).